



Avalanche Studies and Model Validation in Europe, SATSIE

Ryggfonn measurements

Winter 2002/2003 and 2003/2004

20021048-5

November 30, 2004

Client: European Commission
Contact person: Maria Yeroyanni
Contract reference: Contract of 18.10.02

For the Norwegian Geotechnical Institute

Project Manager:


Karstein Lied

Report prepared by:


Peter Gauer
and Krister Kristensen

Reviewed by:


Karstein Lied

Work also carried out by:

Postal address:
Street address:
Internet:

P.O. Box 3930 Ullevaal Stadion, N-0806 OSLO, NORWAY
Sognsveien 72, OSLO
<http://www.ngi.no>

Telephone: (+47) 22 02 30 00
Telefax: (+47) 22 23 04 48
e-mail: ngi@ngi.no

Postal account: 0814 51 60643
Bank account: 5096 05 01281
Business No. 958 254 318 MVA



SUMMARY

This report presents data collected from the full-scale Ryggfonn project during the Winters 2002/2003 and 2003/2004. The weather and snow conditions described and when possible, the avalanches have been characterized according to the IAHS avalanche code and the deposit boundaries have been mapped.

Measurements obtained from the avalanche path include pressure readings from two load cells at a steel tower, as well as avalanche pressure on three load cells fixed to a concrete structure. In addition, normal stress and shear stress were measured on two locations at a 16 high dam. Six geophones, placed on the ground in the runout zone, have detected vibrations from some of the passing avalanches. When possible, for each avalanche the front speeds have been estimated. The estimates are based on continuous-cave Doppler radar measurements, seismic measurements, and the timing between impacts on the constructions.

The measurements obtained are briefly discussed and presented in graphs.



Contents

1 Ryggfonn full-scale experiments (NGI)	4
2 Winter 2002/2003	8
3 Winter 2003/2004	28
Appendix A - International Avalanche Classification	

List of Tables

2.1 Monthly precipitation and air temperature at 930 m a.s.l.	8
2.2 Avalanche classification	8
2.3 Overview of archived measurements at Ryggfonn test site during winter season 2002/2003	10
3.1 Monthly precipitation and air temperature at 930 m a.s.l.	28
3.2 Avalanche classification	28
3.3 Overview of archived measurements at Ryggfonn test site during winter season 2003/2004	30

List of Figures

1.1 Ryggfonn avalanche test site; location map	4
1.2 Drag factor vs Reynolds number for a mud flow hitting a pipe	5
1.3 Relationship between shear stress vs normal stress for various rheological models	6
2.1 Weather data from Fonnbu 2002–2003	9
2.2 Deposition map of avalanches recorded in winter season 2002/2003	10
2.3 Avalanche 20030114 03:30: Load cell measurements	12
2.4 Avalanche 20030114 05:30: Load cell measurements	13
2.5 Avalanche 20030115 13:27: Speed estimates	14
2.6 Avalanche 20030115 13:27: Load cell measurements	15
2.7 Avalanche 20030115 13:27: Load cell measurements, turbulent intensity . .	16
2.8 Avalanche 20030115 13:27: Pressure profile	17
2.9 Avalanche 20030115 13:27: Load plate measurements	18
2.10 Avalanche 20030115 13:27: Deposition map	18
2.11 Avalanche 20030118 15:14: Speed estimates	19
2.12 Avalanche 20030118 15:14: Load cell measurements	20
2.13 Avalanche 20030118 15:14: Load cell measurements, turbulent intensity . .	21
2.14 Avalanche 20030406 13:06: AIATR speed measurements	23
2.15 Avalanche 20030406 13:06: Load cell measurements	24
2.16 Avalanche 20030406 13:06: Load cell measurements, turbulent intensity . .	25
2.17 Avalanche 20030406 13:06: Photo AIATR	26
2.18 Avalanche 20030406 13:06: Snow profiles	27
3.1 Weather data from Fonnbu 2003–2004	29
3.2 Deposition map of avalanches recorded in Winter 2003/2004	30



3.3	Avalanche 20031215 16:40: Speed estimates	32
3.4	Avalanche 20031215 16:40: Load cell measurements	33
3.5	Avalanche 20031215 16:40: Load cell measurements, turbulent intensity . .	34
3.6	Avalanche 20031215 16:40: Pressure profile	35
3.7	Avalanche 20031215 16:40: Load plate measurements	36
3.8	Avalanche 20031217 03:24: Speed estimates	37
3.9	Avalanche 20031217 03:24: Deposition map	38
3.10	Avalanche 20031217 03:24: Load cell measurements	39
3.11	Avalanche 20031217 03:24: Load cell measurements, turbulent intensity . .	40
3.12	Avalanche 20031217 03:24: Pressure vs position within avalanche	41
3.13	Avalanche 20031217 03:24: Pressure profile	42
3.14	Avalanche 20040204 06:10: Speed estimates	43
3.15	Avalanche 20040204 06:10: Deposition map	44
3.16	Avalanche 20040204 06:10: Load cell measurements	45
3.17	Avalanche 20040204 06:10: Load cell measurements, turbulent intensity . .	46
3.18	Avalanche 20040204 06:10: Pressure vs position within avalanche	47
3.19	Avalanche 20040204 06:10: Pressure profile	48
3.20	Avalanche 20040204 06:10: Load plate measurements	49
3.21	Avalanche 20040224 08:50: Speed estimates	50
3.22	Avalanche 20040224 08:50: Load cell measurements	51
3.23	Avalanche 20040224 22:30: Speed estimates	52
3.24	Avalanche 20040224 22:30: Deposition map	53
3.25	Avalanche 20040224 22:30: Load cell measurements	54
3.26	Avalanche 20040224 22:30: Load plate measurements	55
3.27	Avalanche 20040224 22:31: Load cell measurements	56
3.28	Avalanche 20040228 15:30: Speed estimates	57
3.29	Avalanche 20040228 15:30: Deposition/outline map	58
3.30	Avalanche 20040228 15:30: Snow profile	59
3.31	Avalanche 20040228 15:30: Snap shots	60
3.32	Avalanche 20040228 15:30: Deposition pattern	61
3.33	Avalanche 20040228 15:30: Load cell measurements	62
3.34	Avalanche 20040228 15:30: Load cell measurements, turbulent intensity . .	63
3.35	Avalanche 20040228 15:30: Load plate measurements	64

1 Ryggfonn full-scale experiments (NGI)

Task leader: Karstein Lied; participation of Krister Kristensen, Carl Harbitz, Peter Gauer, Arne Moe, Erik Lied and Harald Iwe, as well as the Department of Geology and Geophysics, University of Barcelona, the Icelandic Meteorological Office - Avalanche section and Austrian Institute for Avalanche and Torrent Research

The Ryggfonn full-scale avalanche test site has been in operation since 1980. The test site has a vertical drop of about 900 m and a horizontal length of 2100 m. Typical avalanche size ranges between 2 (mass of 0.1 Gg) and 4 (mass of 10 Gg) according to the Canadian snow avalanche size classification (McClung and Schaerer, 1993), and maximum velocity up to 60 m s^{-1} . Figure 1.1 shows a location map of the main sensors used during the winter season 2003/2004.

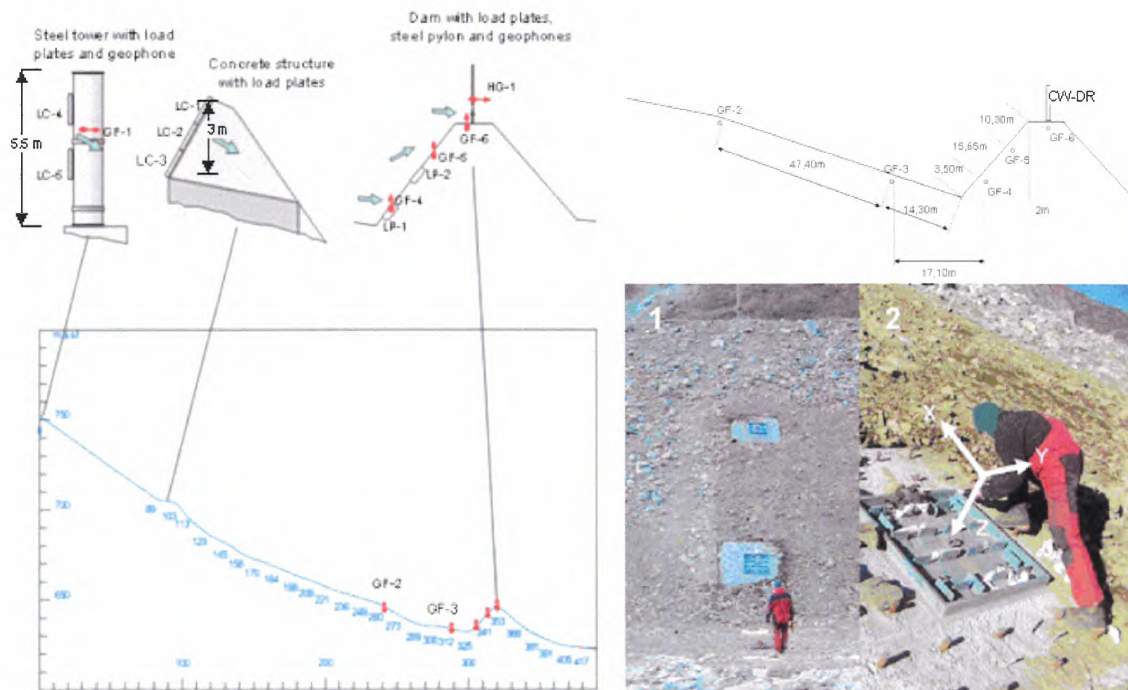


Figure 1.1: Ryggfonn avalanche test site; location map. Left panel shows an overview and right panels give close ups of the dam area. Lower right figure shows the definition of the co-ordinate direction of the load plates at the dam

The steel tower has a diameter 1.3 m and is equipped with 2 load plates, each with an area, A_m , of $1.2 \text{ m} \times 0.6 \text{ m}$. The concrete structure is instrumented with 3 load plates identical to those at the steel tower. The force on given plate might be written as

$$F_{LC} = \rho_{av} C_D A_a \frac{U^2}{2}, \quad (1.1)$$

where ρ_{av} is the density of the flowing avalanche, U its speed, and C_D a drag factor. The drag factor is not a constant. It rather depends on the geometry of the obstacle

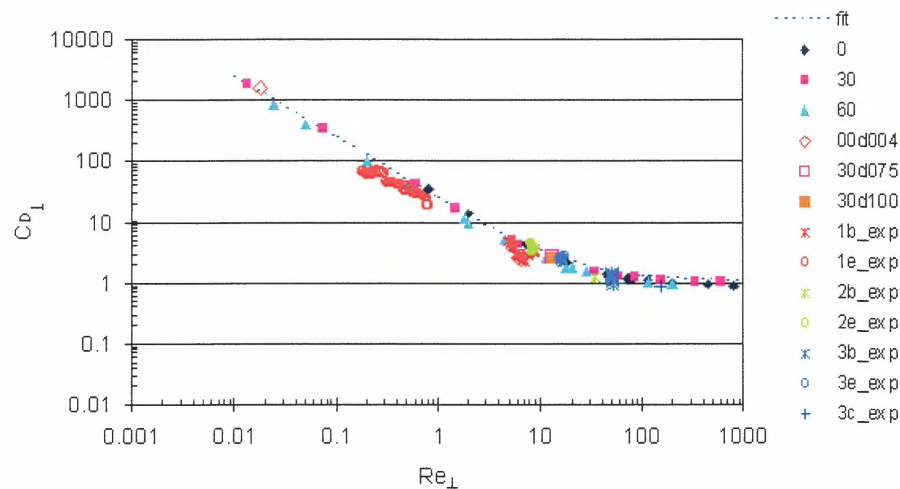


Figure 1.2: Drag factor vs Reynolds number for a mud flow hitting a pipe; compilation of experiments and simulations, $Re = d U^2 / Y$, where d is the diameter, U the velocity, and τ_c the shear strength.

(sensor configuration), the flow regime, and might depend on the snow properties within the avalanche, see for example Figures 3.12 or 3.18. This fact should be borne in mind when evaluating the load cell measurements. How C_D might change depending on the flow regime shows an example of the drag factor for a mud flow hitting a pipe (see Fig 1.2).

A_a is the affected area hit by the avalanche. If A_a is less A_m then the pressure measurements have to be corrected by a (unknown) factor A_m/A_a . This can cause an uncertainty, e.g., by the defining of the profile in Figures 3.6, 3.13, and 3.19. Reasons for $A_a < A_m$ can be that the flow height of the avalanche is smaller than the height of the plate or the plate is already buried from deposits.

Due to the large size of the sensors, the measured impact forces represent average values. Single impacts might exceed this values by an order of magnitude. The averaging effect of the large size also causes a damping of the turbulent intensity presented in, e.g., Figures 3.5, 3.11, and 3.17. Here, the turbulent intensity is a measure for the fluctuation in pressure recordings and is affected by, e.g., velocity and density fluctuations. It is defined as

$$ILC = \left| \frac{LC - \overline{LC}}{\overline{LC}} \right|. \quad (1.2)$$

LC is the measured pressure by the load cell and \overline{LC} is a running mean taken either over 0.5 s (approximately between 5 m to 15 m spatial resolution) or 5 m. Temporal averaging has the disadvantage that the spatial resolution might change during time. However, spatial averaging seems also only reasonable, if at least a rough estimate of the velocity distribution along the flow direction is available. For a better comparison, the plots of the turbulent intensity are restricted to a maximum value of one, even if partly this value is exceeded.

The two load plates, LP , in the dam are mounted flush with the slope surface. Hence, in an unsupported static case the relation

$$\frac{LP_X}{LP_Z} = -\tan \psi_D = -0.84 \quad \text{and} \quad LP_Y = 0 \quad (1.3)$$

holds, where the dam slope angle $\psi_D = 40^\circ$. During an avalanche passage, relation for the total shear stress $LP_{XY} = \sqrt{LP_X^2 + LP_Y^2}$ depends on the rheological behavior of the flowing avalanche and on that of the snowpack. For various avalanche models one would get

$$LP_{XY} = \begin{array}{l} \text{plastic type} \\ \tau_c \end{array} \left| \begin{array}{l} \text{Coulomb type} \\ \mu LP_Z \end{array} \right| \begin{array}{l} \text{Voellmy type} \\ \mu LP_Z + \frac{\rho_{av}}{\xi} U^2 \end{array}, \quad (1.4)$$

here τ_c is a limit shear strength depending either of the flowing avalanche or the strength of the snowpack. μ is a friction coefficient, and ξ a drag coefficient. Figure 1.3 illustrates how LP_{XY} would depend on LP_Z for the different models. All measurements so far range at the low end of the sensor range and might be affected by the low sensor sensitivity.

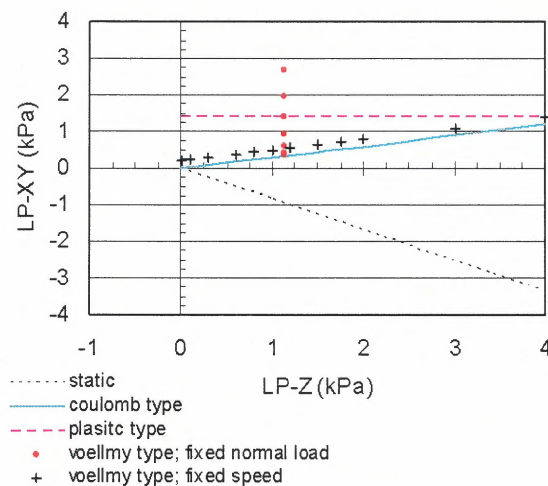


Figure 1.3: Relationship between shear stress, LP_{XY} , vs normal stress, LP_Z , for various rheological models, here the total shear stress $LP_{XY} = \sqrt{LP_X^2 + LP_Y^2}$.

Estimates of the avalanche front speed are based on continuous-wave Doppler radar (CW-DR) measurements by the Icelandic Meteorological Office (IMO), seismic measurements by the Department of Geology and Geophysics (DGG) at the University of Barcelona, and the timing between impacts on the constructions. The evolution of the radar data with respect to the track position is based on work done by Ignasi Vilajosana Guillen (DGG). The different methods bear a wide range of uncertainties, e.g., the radar velocity spectra are taken over a spatial window of approximately 300 m. Hence, the tracking of the avalanche front is rather uncertain. For that reason, care should be taken regarding the interpretation of the radar data. Also the estimates based on impacts have different sources for errors, e.g., the avalanche might hit the steel tower with a first wave, but miss the concrete structure. When a second wave now hits the concrete structure the measured



time difference causes an underestimation of the front speed. Also the identification of the impact on the sensor is not straight forward and afflicted with uncertainties. Estimates based on timing of measurements between two sensors are taken as the average over the distance and displayed at the horizontal mid point.

In the plot for time series, the zero time is taken as the time when the avalanche hits the first sensor. In Winter 2002/2003 the first sensor was the concrete structure and in Winter 2003/2004 the steel tower.



2 Winter 2002/2003

General conditions in 2002/2003 The winter 2002/2003 had unusually stable weather and comparatively small amounts of snow. Despite of this, data from one cycle of natural avalanches and one artificially released avalanche were obtained. In addition one avalanche released during blasting of residual explosives in May. Table 2.2 gives an overview of the avalanches and Figure 2.2 show the outline of two of those. A summary of the weather conditions is given in Table 2.1 and Figure 2.1.

Table 2.1: Monthly precipitation and air temperature at 930 m a.s.l.

2002/2003	Precip. mm	Air temperature °C		
		mean	max	min
December	N/A	-7.4	1.8	-17.7
January	N/A	-4.9	5.2	-18.8
February	12.4	-3.7	5.1	-13.2
March	59.4	-2.3	4.9	-13.4
April	41.2	0.4	7.7	-7.9
May	N/A	2.6	9.2	-7.7

Table 2.2: Avalanche classification

Date yyyymmdd hh:mm	Release	Size ¹	Type	Classification (ICSI) ² A B C D E F G H J	Speed (m s ⁻¹)	
					LC4-LC1 ³ (100 m)	LC1-LP1 ⁴ (218 m)
20030111 11:00	natural	2	dry	// 1 // // // // 1	-	-
20030114 03:30	natural	3	dry	// 1 // // // // 1	-	-
20030114 05:40	natural	3	dry	// 1 // // // // 1	-	-
20030115 13:27	natural	3.5	dry	2 / 7 // / 3 // / 1	-	31
20030118 15:14	natural	3	wet/flow	3 2 2 2 7 3 1 1 1	-	4.4
20030406 13:06	artificial	3	dry/mixed	3 2 1 2 7 3 1 1 4	13.5	-

¹According to Canadian avalanche size classification.

²According international avalanche classification (Avalanche Atlas UNESCO/IAHS, 1981).

³Speed estimate from AIATR Doppler radar measurements.

⁴The estimated averaged speed are calculated between the concrete structure and the foot of the dam.

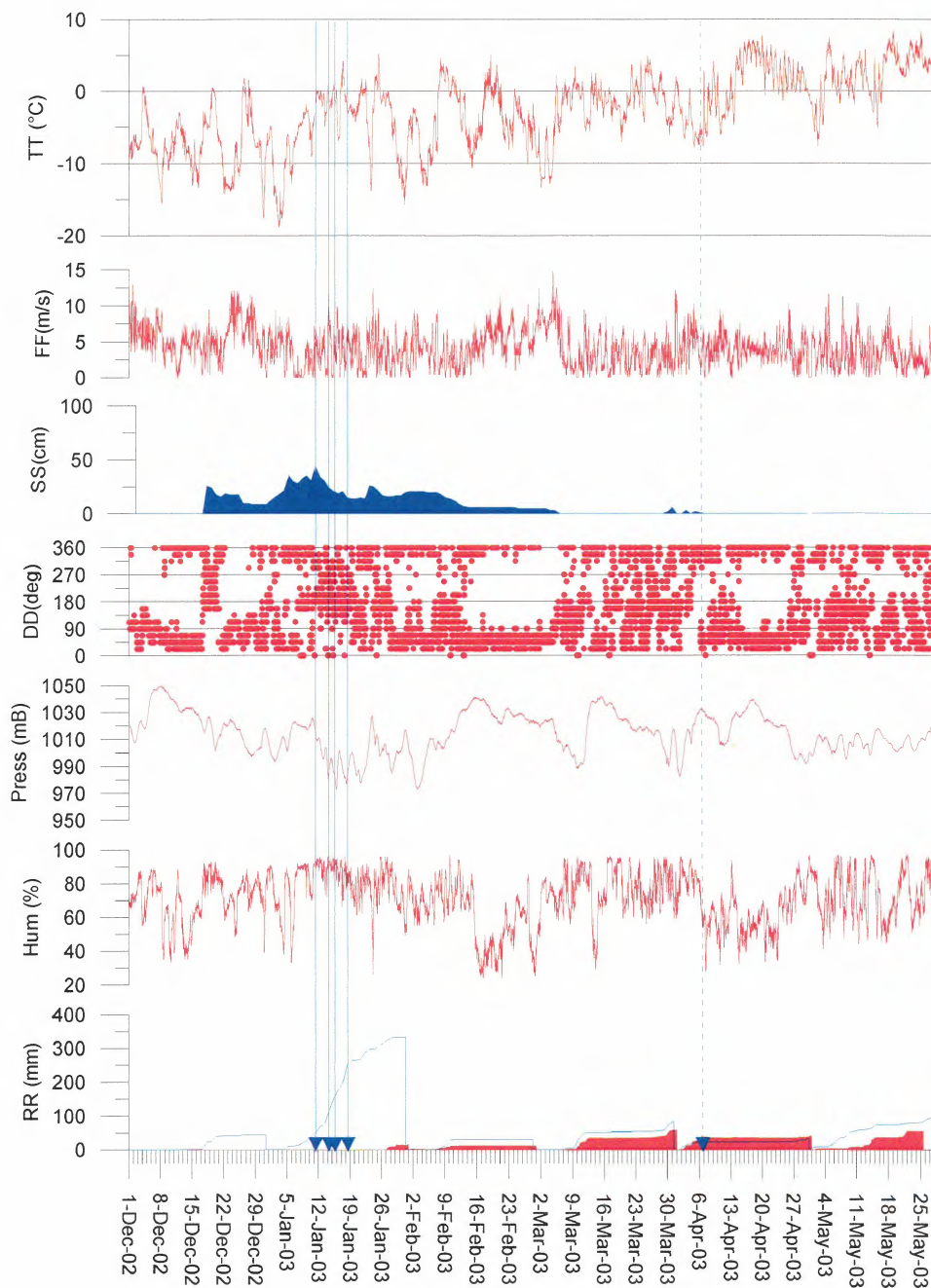


Figure 2.1: Weather data from Fonnbu 930 m a.s.l. The snow height and the unfilled accumulated precipitation graphs is based on data from the DNMI-station 58880 Sindre, 118 m a.s.l. Vertical lines with arrows indicate avalanches in Ryggfonn (solid=natural, dotted=artificial avalanche)

Table 2.3: Overview of archived measurements at Ryggfonn test site during winter season 2002/2003

Date yyyymmdd hh:mm	geophone (GF)1 2 3 4 5 6 H1	load cell (LC)4 5 1 2 3	load plate (LP)1 2	radar AIATR	field obs.	maps
20030111 11:00	- - - - -	- - X X X	- -	-	-	-
20030114 03:30	- X X X X X -	- - X X X	- -	-	-	-
20030114 05:40	- X X X X X -	- - X X X	U U	-	-	-
20030115 13:27	- X X X X X X	- - X X X	X U	-	X	X
20030118 15:14	- X X X X X X	- - X X X	X U	-	-	-
20040406 13:06	- O O O O O O	- - X X X	O O	X	X	X

Codes: X -data; P -sensor partly buried; B -sensor buried; O -data, but no measured signal (did not reach sensor); - -no data; U -sensor status unknown

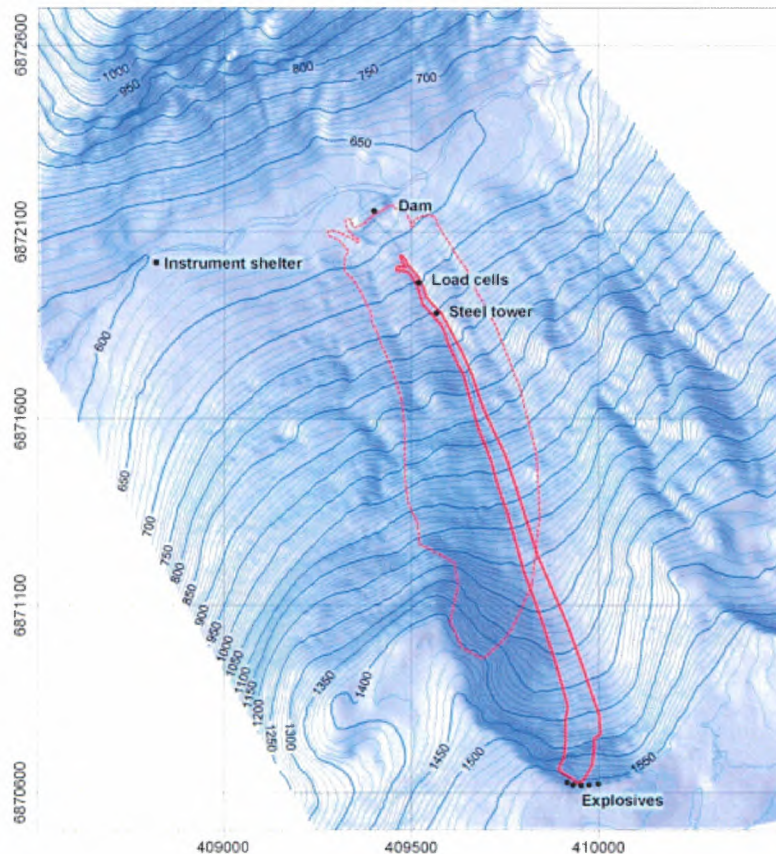


Figure 2.2: Map of the Ryggfonn test site with the avalanches recorded in Winter 2002/2003. The dotted line indicates the natural avalanche recorded on January 15th, while the solid line represents an artificially released avalanche on April 6th



Avalanches during January 2003

Weather and avalanche summary During a period of strong winds and snow from January 11th to 18th, several natural avalanches ran in the Ryggfonn path and the adjacent area. The largest avalanche in this period occurred on January 15th at 13:27 h. Because the 0°C isotherm was at around 1000 m a.s.l. at the time of release, the avalanche consisted of partly wet snow. As can be seen from the photo (see 2.10) the avalanche originated from the west side of the cirque and lower on the west ridge. Bad visibility and irregular terrain made it difficult to estimate the depth and extent of the initial fracture. A rough estimate of the mean fracture height would be around 1.5 m. The areal extent of the initial slab would be around 50,000 m² (horizontal projection). However, it is evident that some entrainment of the loose, wet snow in the lower path has taken place. The volume of the deposit in the run-out zone below the load cells on the concrete structure is estimated to around 120,000 m³.

Avalanche 20030114 03:30

Avalanche code (UNESCO/IAHS 1981): A/, B/, C1, D/, E/, F1, G/, H/, J1

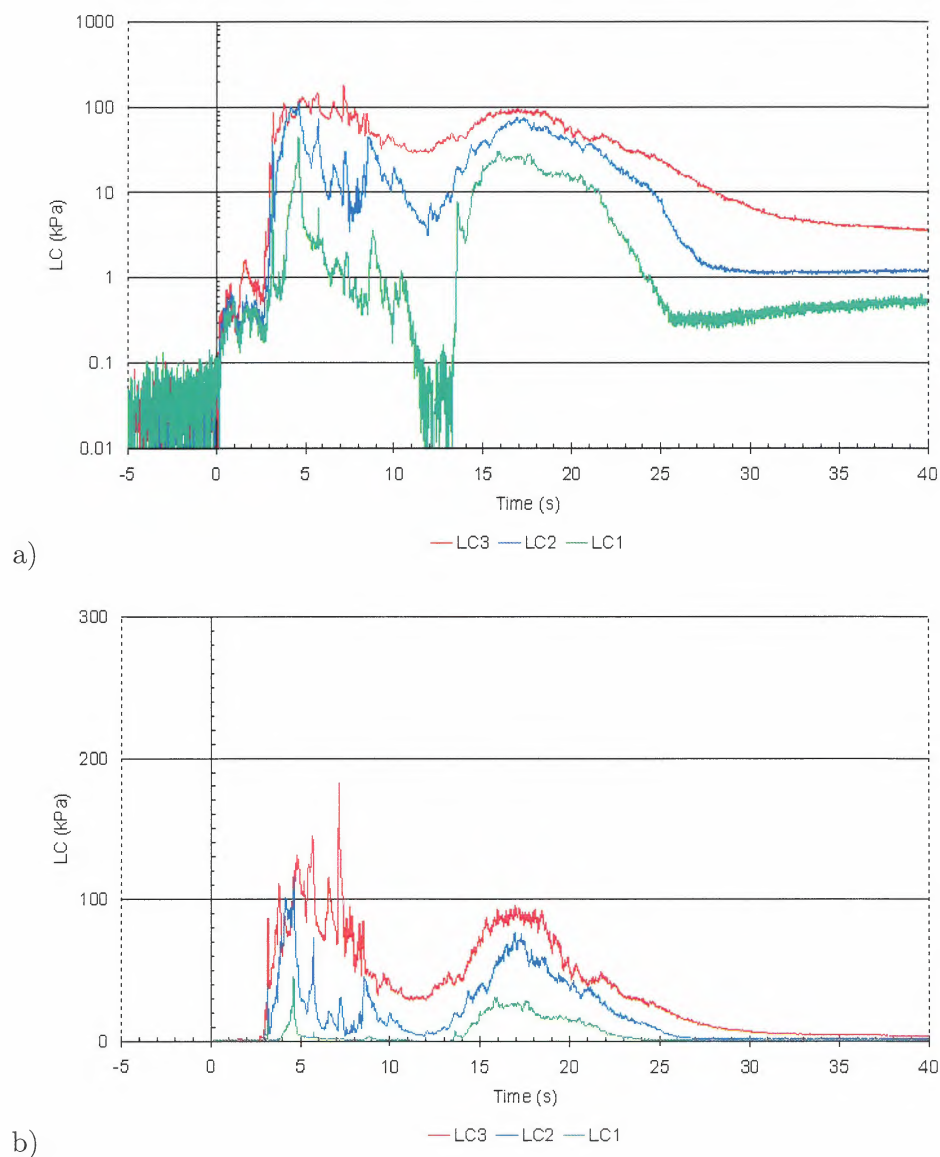
Results

Figure 2.3: *Avalanche 20030114 03:30: Load cell measurements: pressure vs time; a) logarithmic and b) linear presentation.*

Avalanche 20030114 05:30

Avalanche code (UNESCO/IAHS 1981): A/, B/, C1, D/, E/, F1, G/, H/, J1

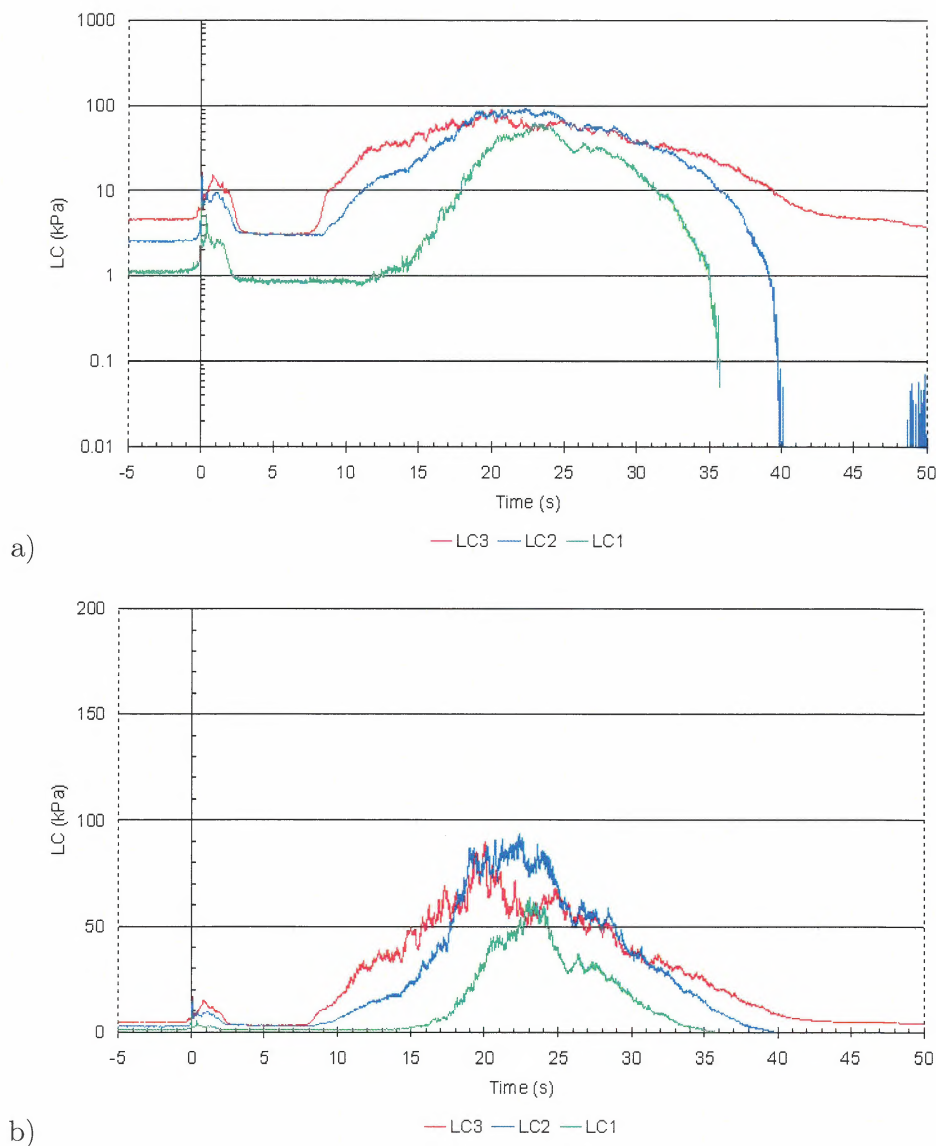
Results

Figure 2.4: Avalanche 20030114 05:30: Load cell measurements: pressure vs time; a) logarithmic and b) linear presentation.

Avalanche 20030115 13:27

Avalanche code (UNESCO/IAHS 1981): A/, B/, C7, D/, E/, F3, G/, H/, J1

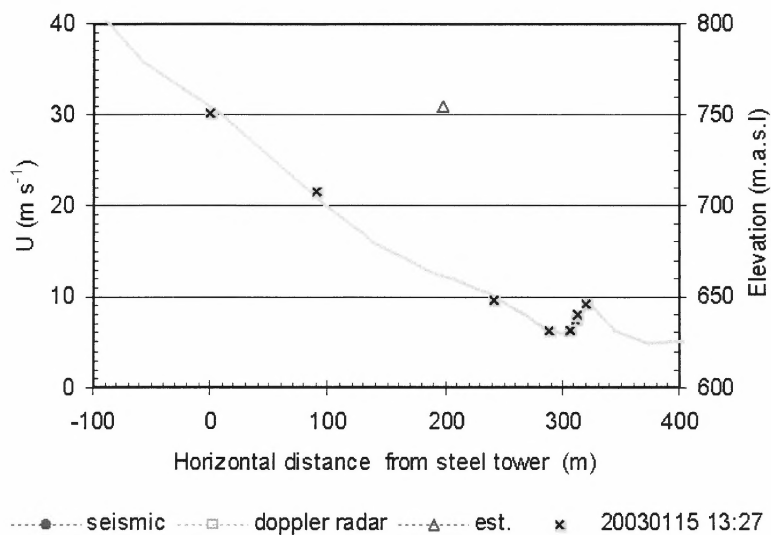
Results

Figure 2.5: *Avalanche 20030115 13:27: Estimated averaged front velocity between various sensors (marked by \boxtimes).*

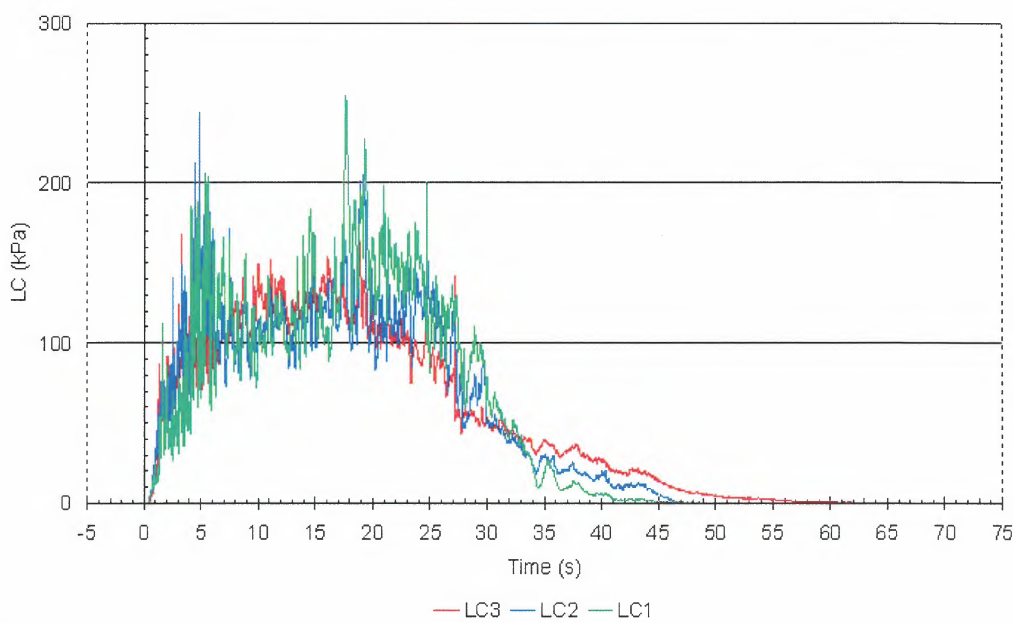
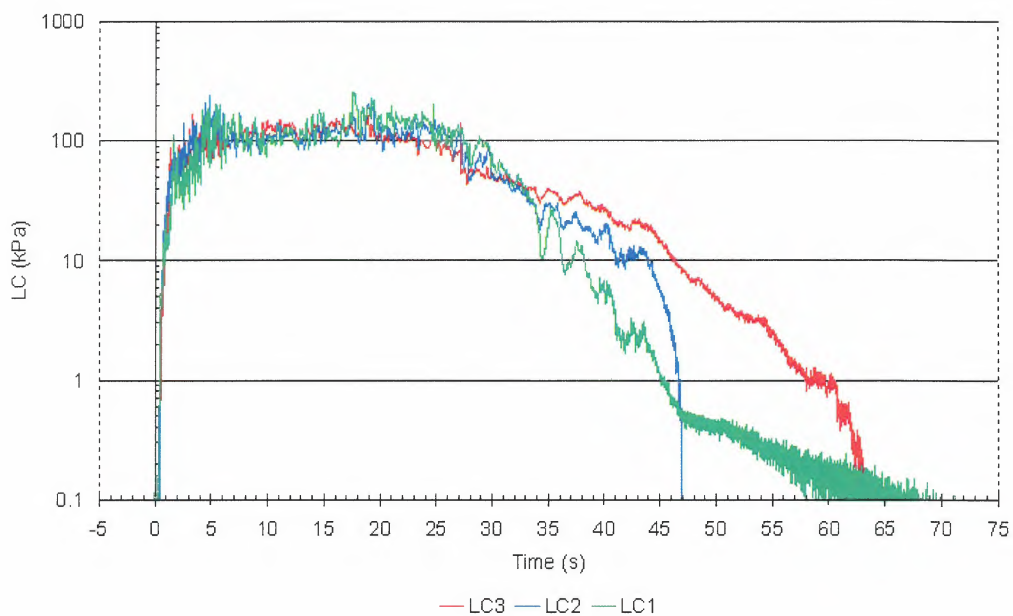


Figure 2.6: *Avalanche 20030115 13:27: Load cell measurements: pressure vs time; a) logarithmic and b) linear presentation.*

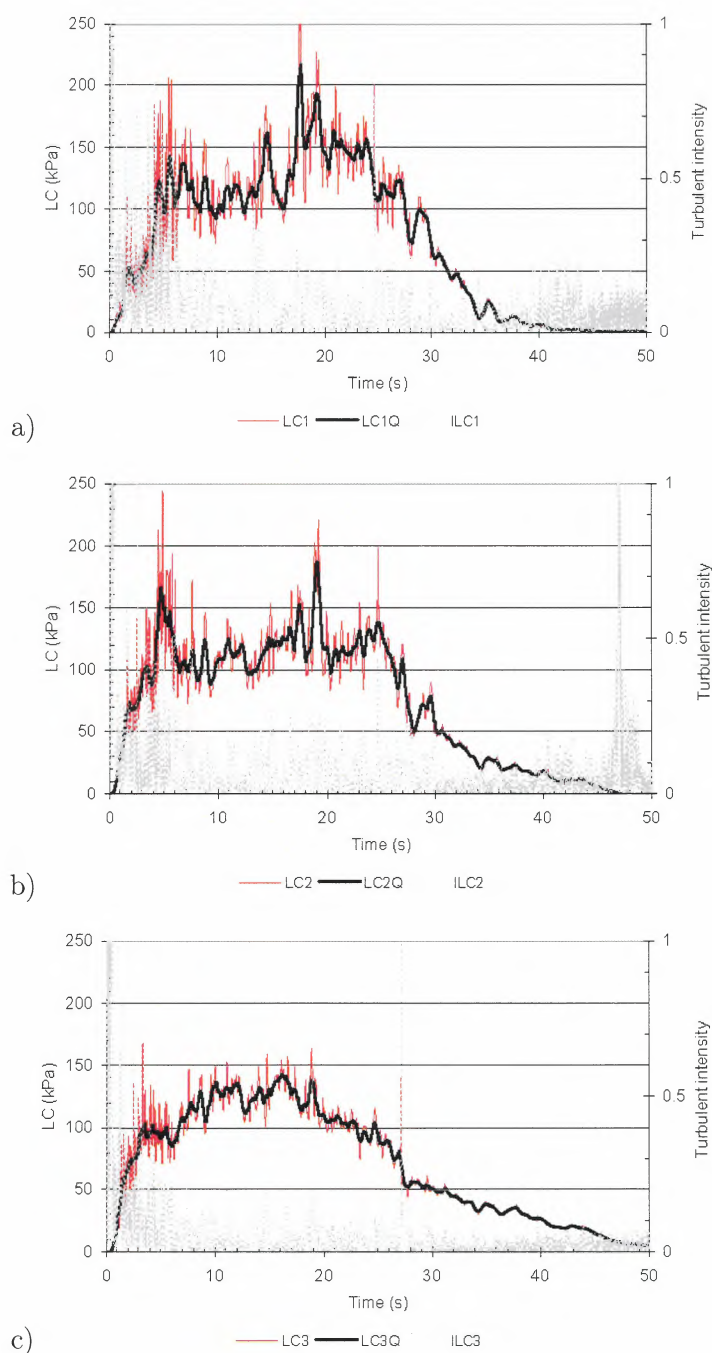


Figure 2.7: *Avalanche 20030115 13:27: Load cell measurements: pressure vs time; shown is the measured value (LCX) and a running mean (LCXQ) taken over 0.5 s (approximately between 5 m to 15 m spatial resolution). In addition, the turbulent intensity is presented (see Eq. (1.2) for definition). Obvious is the high turbulent intensity at the front of the avalanche and in the upper part indicating a high fluidization. a) LC1, b) LC2, and c) LC3. Remarkably is the low vertical gradient, indicating a rather high flow height.*

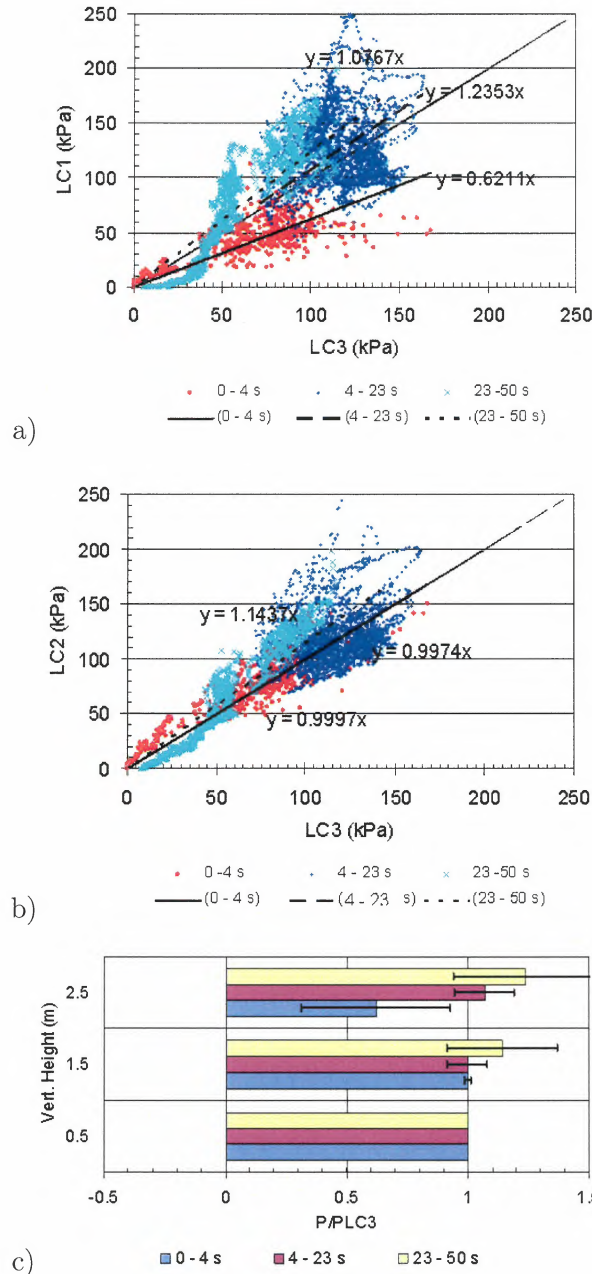


Figure 2.8: Avalanche 20030115 13:27: a) and b) show a plot of $LC1$ and $LC2$ vs $LC3$, respectively, and linear trends for different time periods. c) presents a normalized pressure profile for the different time periods. Assuming a negligible vertical velocity gradient, the profile is an indication of the density profile within the avalanche. However some care has to be taken as the ration A_a/A_m is not known. The error bars mark the relative error from the linear relation $(LC_X - a LC_3)/(a LC_3)$, here a is the slope of the linear interpolation. High errors indicate also high fluctuations. Remarkably is the low vertical gradient, indicating a rather high flow height.

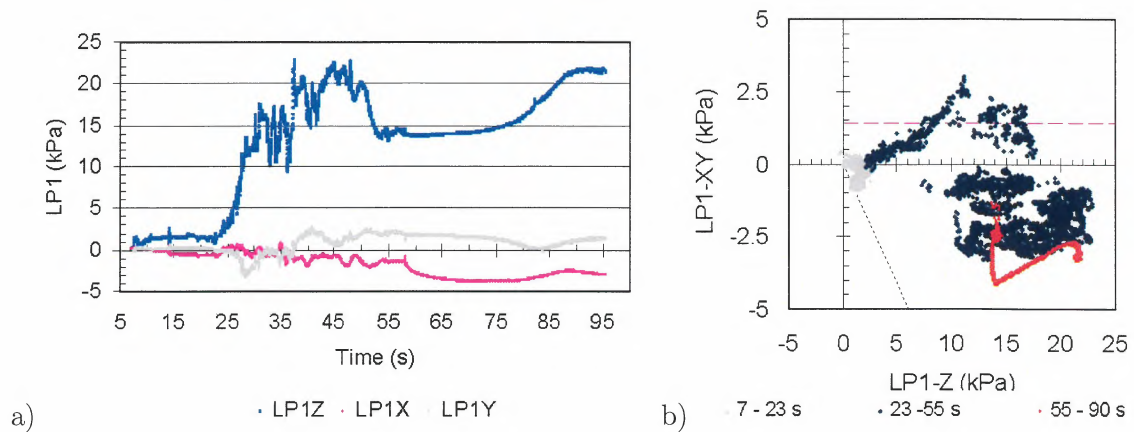


Figure 2.9: Avalanche 20030115 13:27: Load plate measurements; a) LP1 vs time; b) LP1-XY vs LP1-Z; here LP1-XY is the total shear stress and the sign indicates its direction parallel to the x-axis (see Fig. 1.1).



Figure 2.10: Avalanche 20030115 13:27: Deposit of the January 15th avalanche. Photo taken from the dam crest



Avalanche 20030118 15:14

Avalanche code (UNESCO/IAHS 1981): A3, B2, C2, D2, E7, F3, G1, H1, J1.

Weather and avalanche summary January 18: At 930 m a.s.l the air temperature was -9.6°C , with high temperatures of -0.5°C the preceding 24 hours. SW-wind of 6.3 m s^{-1} , with gusts up to 21 m s^{-1} .

Results

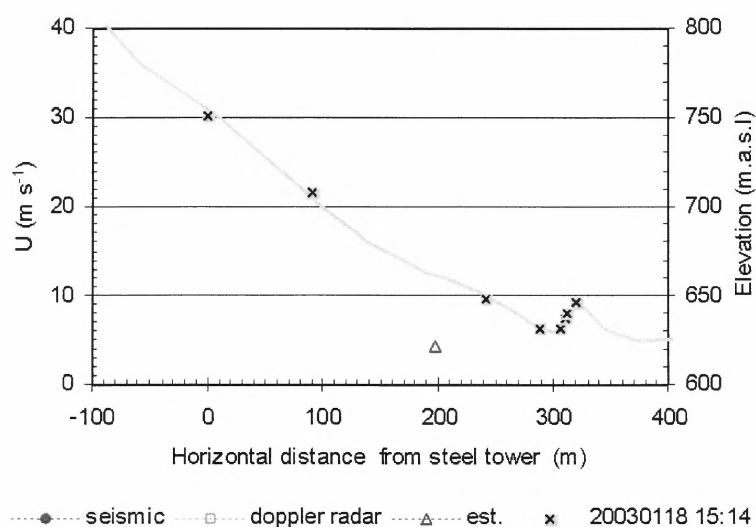


Figure 2.11: *Avalanche 20030118 15:14: Estimated averaged front velocity between various sensors (marked by \boxtimes).*

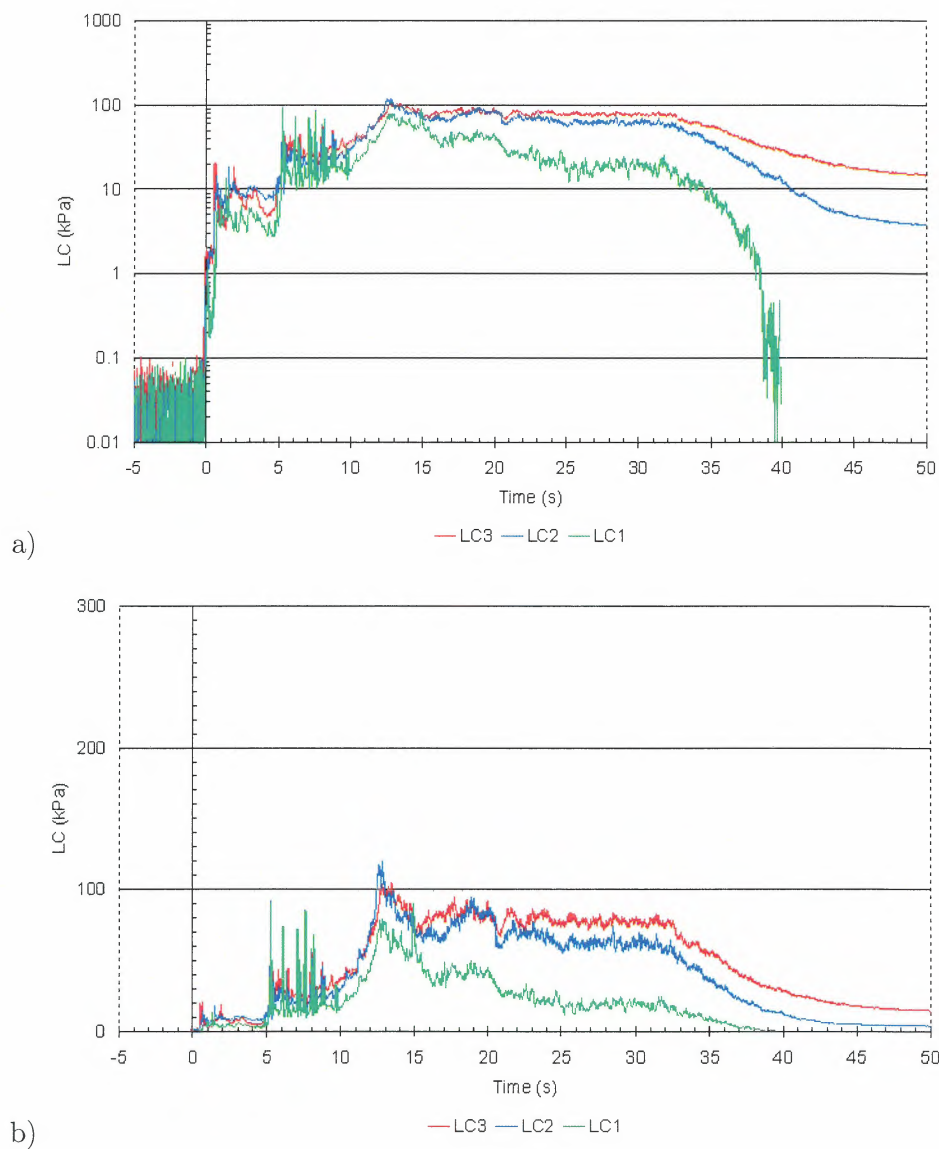


Figure 2.12: *Avalanche 20030118 15:14: Load cell measurements: pressure vs time; a) logarithmic and b) linear presentation.*

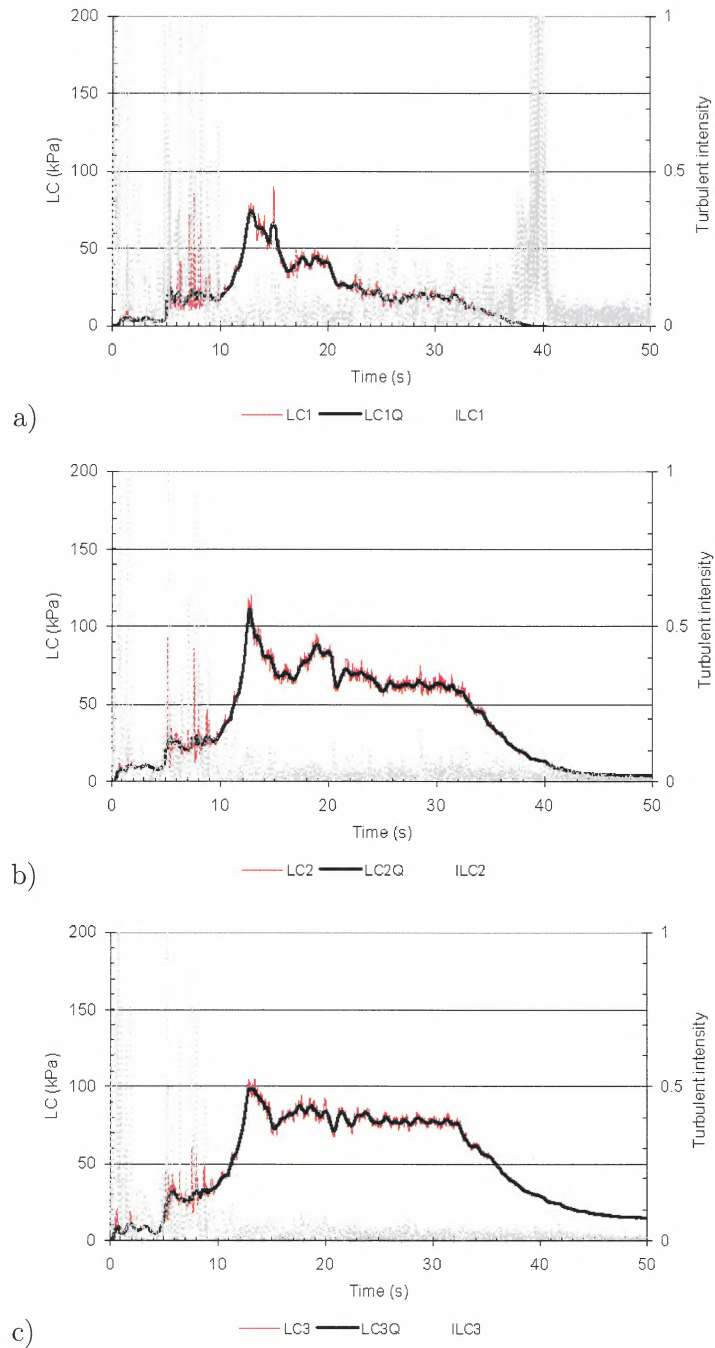


Figure 2.13: *Avalanche 20030118 15:14: Load cell measurements: pressure vs time; shown is the measured value (LCX) and a running mean (LCXQ) taken over 0.5 s (approximately between 5 m to 15 m spatial resolution). In addition, the turbulent intensity is presented (see Eq. (1.2) for definition). Obvious is a high turbulent intensity at the front of the avalanche. In the main body, the fluctuation are rather low. a) LC1, b) LC2, and c) LC3. Remarkably is the low vertical gradient between LC3 and LC2, indicating a rather high flow height.*



Avalanche 20030406 13:06

Avalanche code (UNESCO/IAHS 1981): A3, B2, C1, D2, E7, F3, G1, H1, J4.

Weather and avalanche summary Following the mid-January storm period, there was unusually little precipitation in Western Norway: Despite the fact that the snow cover was rather unstable because of depth hoar formation in the early winter, no further natural avalanches were released. After a brief period of snowy weather in the beginning of April, it was decided to try to release artificially an avalanche on April 6th. The release was triggered by detonating 150 kg of pre-placed explosives buried under the massive cornice at the top of the starting zone. The resulting avalanche was comparatively small, but it did reach the load cells in the lower path. However, it stopped about 150 m short of the dam. The avalanche was released during dry snow conditions with fresh wind slab formation in the starting zone. In the lower half of the path, most of the snow pack consisted of melt-freeze metamorphosed snow, covered by about 10 cm of dry new snow at the top. The initial slab had an area of about 18,000 m² (horizontal projection) and the crown height was about 1 m. Because of the more stable snow in the lower part of the path, entrainment gradually decreased and there was a loss of mass before the avalanche reached the measurement devices. Only a small fraction of the mass was able to pass the concrete structure.

At 930 m a.s.l the air temperature was -6.0°C, with high temperature of -5.7°C the preceding 24 hours. Easterly breeze and fairly calm weather.



Results

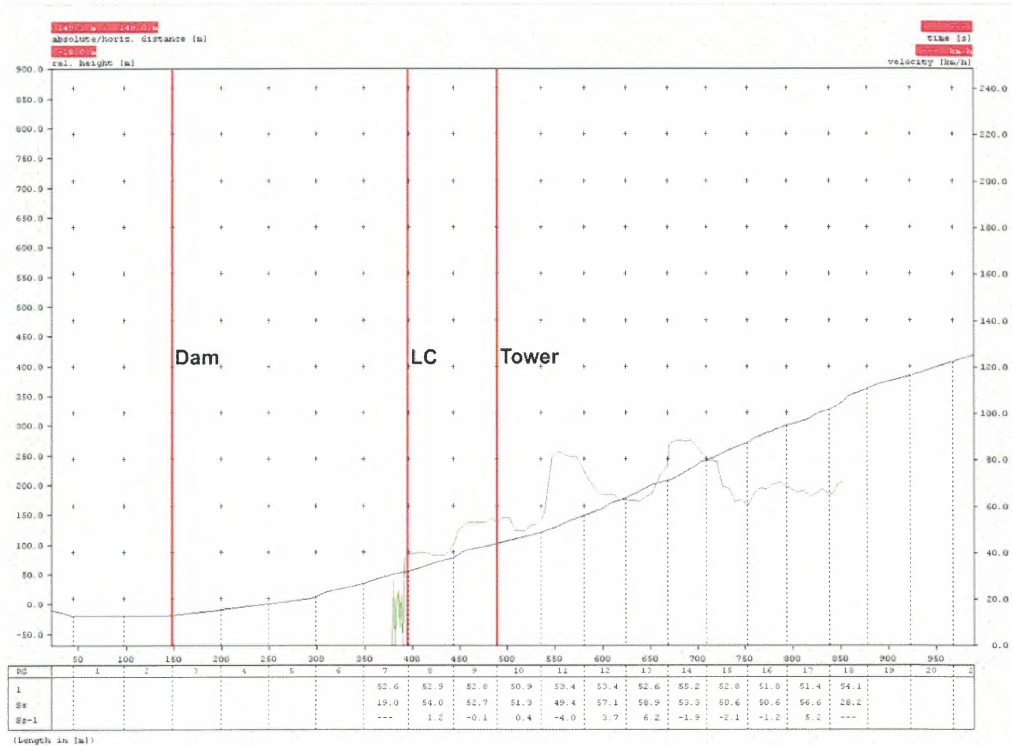


Figure 2.14: Avalanche 20030406 13:06: AIATR Doppler radar measurements of the avalanche.

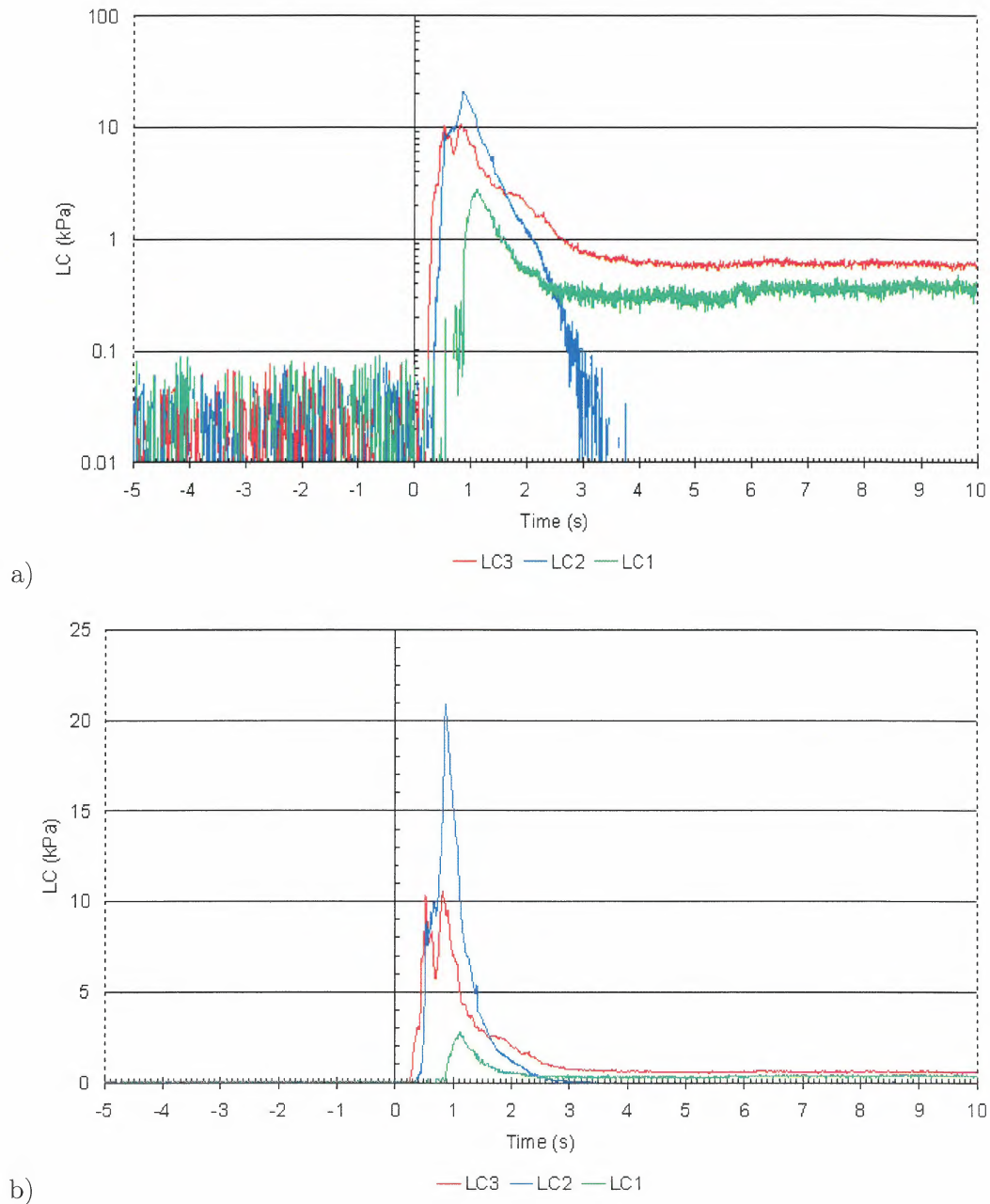


Figure 2.15: Avalanche 20030406 13:06: Load cell measurements: pressure vs time; a) logarithmic and b) linear presentation.

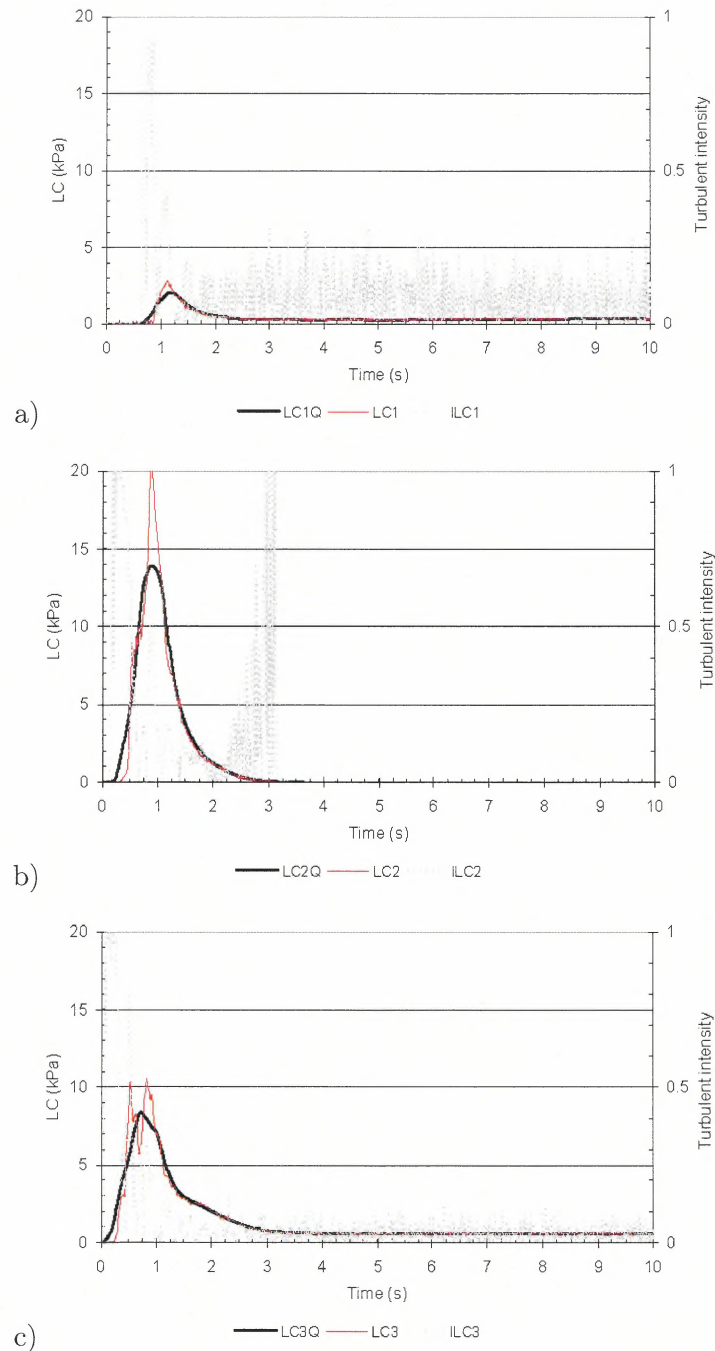


Figure 2.16: Avalanche 20030406 13:06: Load cell measurements: pressure vs time; shown is the measured value (LCX) and a running mean ($LCXQ$) taken over 0.5 s (approximately between 5 m to 10 m spatial resolution). In addition, the turbulent intensity is presented (see Eq. (1.2) for definition) In the tail part, the high turbulent intensity is partly caused by the sensor noise. a) $LC1$, b) $LC2$, and c) $LC3$.

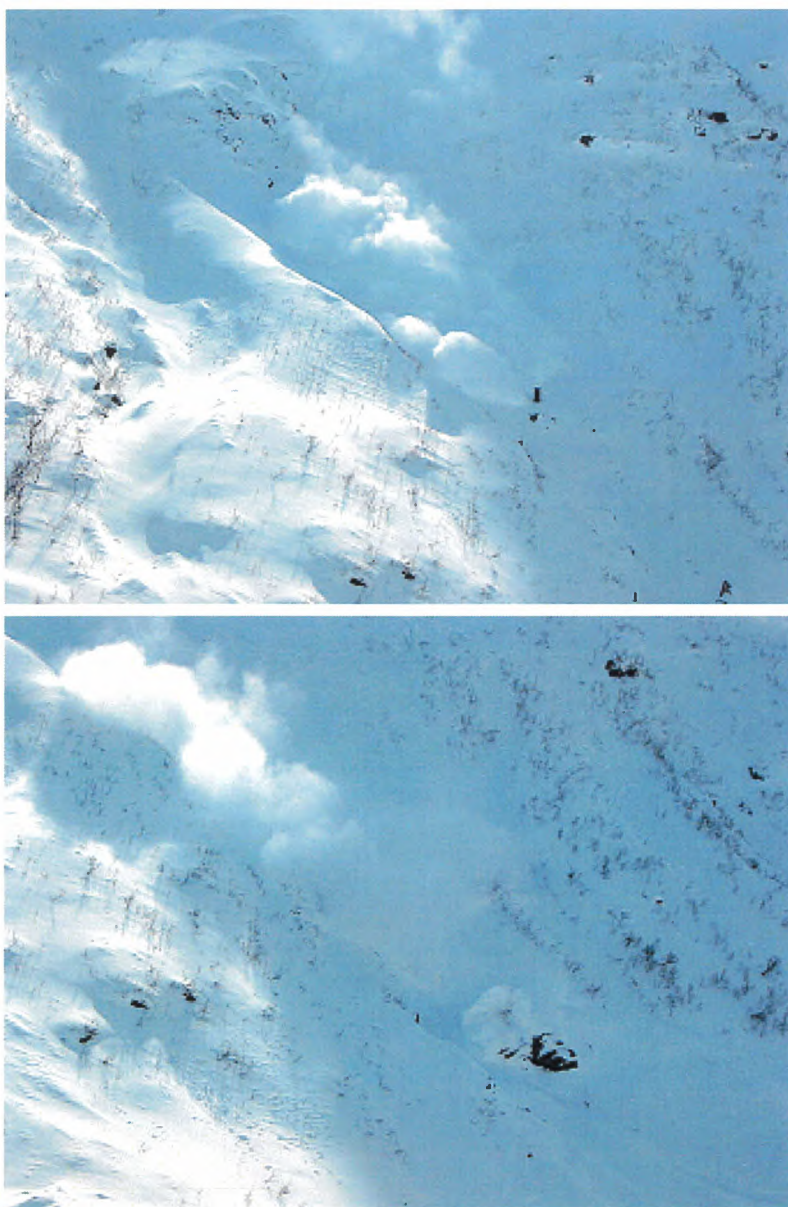


Figure 2.17: *Avalanche 20030406 13:06: Impact of the April 6th avalanche on the steel tower (top) and the concrete structure (bottom). Photo AIATR.*

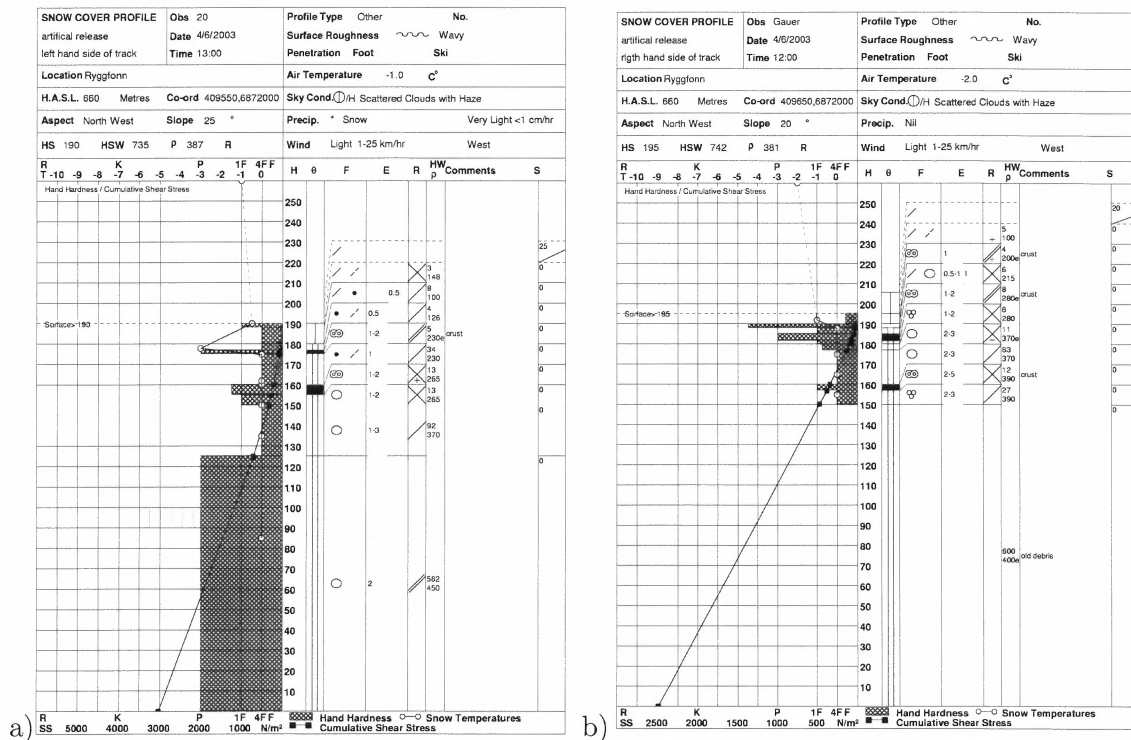


Figure 2.18: Avalanche 20030406 13:06: Snow profile a) left and b) right of the track



3 Winter 2003/2004

General conditions in 2003/2004 In Winter 2003/2004, eight avalanche events were recorded, of which seven were natural releases and one avalanche was artificially triggered.

The 2003/04 winter had somewhat less precipitation and snow on the ground than normal in the Ryggfonn area. Nevertheless, several natural avalanches occurred in December and February. Many of the avalanches released during severe weather conditions. For example, within less than 24 hours, three avalanches ran in the path on February 24-25. All of the naturally released avalanches were monitored by the automatic recording system, although the data obtained from the very first avalanche in December are weak and somewhat ambiguous. Table 3.2 gives a brief classification of the events and Table 3.3 summarizes the conducted measurements for the individual events and an estimation on the sensor status during the event. Figures 3.3 through 3.35 present measurements and results of the avalanches. A summary of the weather conditions is given in Table 3.1 and Figure 3.1.

Table 3.1: Monthly precipitation and air temperature at 930 m a.s.l.

2002/2003	Precip. mm	Air temperature °C		
		mean	max	min
December	198.6	-4.0	4.6	-14.5
January	108.8	-6.8	4.3	-19.6
February	253.9	-4.4	7.4	-16.4
March	54.4	-3.1	6.5	-12.7
April	172.4	1.8	7.5	-6.4
May	38.8	3.0	12.6	-7.3

Table 3.2: Avalanche classification

Date yyyymmdd hh:mm	Release	Size ¹	Type	Classification (ICSI) ² A B C D E F G H J	Speed (m s ⁻¹)	
					LC4-LC1 ³ (100 m)	LC1-LP1 ⁴ (218 m)
20031204 15:19	natural	–	dry ⁵	3 2 7 2 7 / 7 1 1	–	–
20031215 16:40	natural	3	dry/mixed	1 2 1 2 7 4 1 1 1	28	22
20031217 03:24	natural	3	dry/mixed	1 2 1 2 7 4 7 1 1	29	–
20040204 06:10	natural	3.5	wet/flow	1 2 7 2 7 3 2 4 1	22	2.8
20040204 06:12	natural	–	wet/flow	–	6.5	3
20040224 08:50	natural	2	dry/mixed	1 2 1 2 7 4 1 1 1	21	–
20040224 22:30	natural	3	dry/mixed	1 2 1 2 7 4 1 1 1	25	29
20040224 22:31	natural	3	dry/mixed	–	26	19
20040225 02:25	natural	–	dry/mixed	1 2 1 2 7 4 1 1 1	–	–
20040228 15:30	artificial	3.5	dry/mixed	1 2 1 2 7 4 2 1 4	31	18

¹According to Canadian avalanche size classification.

²According international avalanche classification (Avalanche Atlas UNESCO/IAHS, 1981).

³The estimated averaged speed are calculated between the steel tower and the concrete structure,

⁴and between the concrete structure and the foot of the dam, respectively.

⁵Unconfirmed.

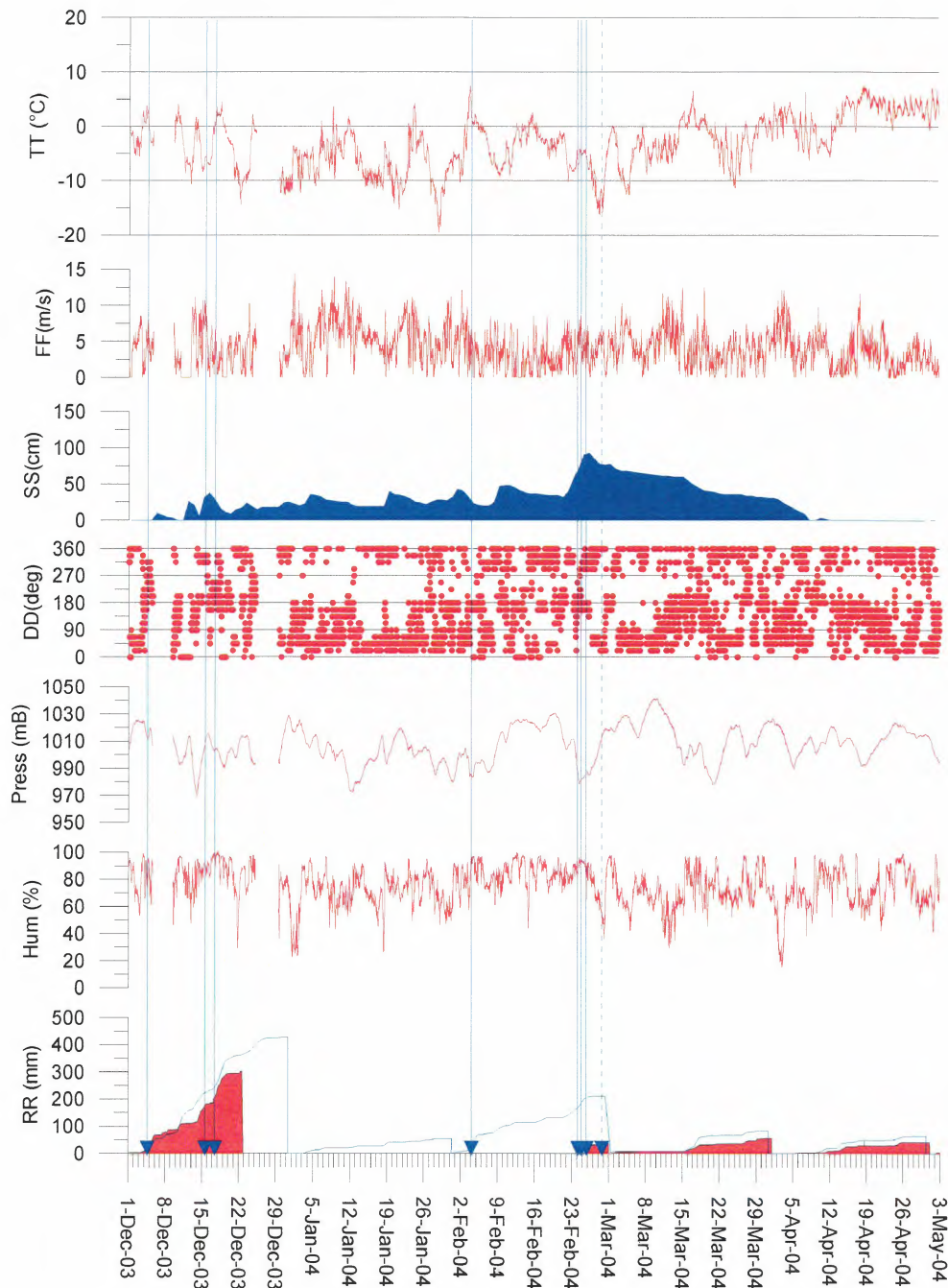


Figure 3.1: Weather data from Fonnbu 930 m a.s.l. The snow height and the unfilled accumulated precipitation graphs is based on data from the DNMI-station 58880 Sindre, 118 m a.s.l. Vertical lines with arrows indicate avalanches in Rygffonn (solid=natural, dotted=artificial avalanche)

Table 3.3: Overview of archived measurements at Ryggfonn test site during winter season 2003/2004

Date yyyymmdd hh:mm	geophone (GF)1 2 3 4 5 6 H1	load cell (LC)4 5 1 2 3	load plate (LP)1 2	radar CW-DR	field obs.	maps
20031204 15:19	- - - - -	- - - - -	- -	-	-	-
20031215 16:40	X X X X X X X	X X X X X	X X	X	-	-
20031217 03:24	X X X X X X X	X P X X X	O O	X	-	X
20040204 06:10	X X X X X X X	X B X X P	X O	-	-	-
20040204 06:12	X X X X X X X	X B X X P	X O	-	X	X
20040224 08:50	X X X X X X X	X B P B B	O O	X	-	-
20040224 22:30	X X X X X X X	X B P B B	X X	X	-	-
20040224 22:31	X X X X X X X	X B P B B	U U	X	-	X
20040225 02:25	- - - - -	- - - - -	- -	-	-	-
20040228 15:30	X X X X X X X	X B P B B	X U	-	X	X

Codes: X -data; P -sensor partly buried; B -sensor buried; O -data, but no measured signal (did not reach sensor); - -no data; U sensor status unknown

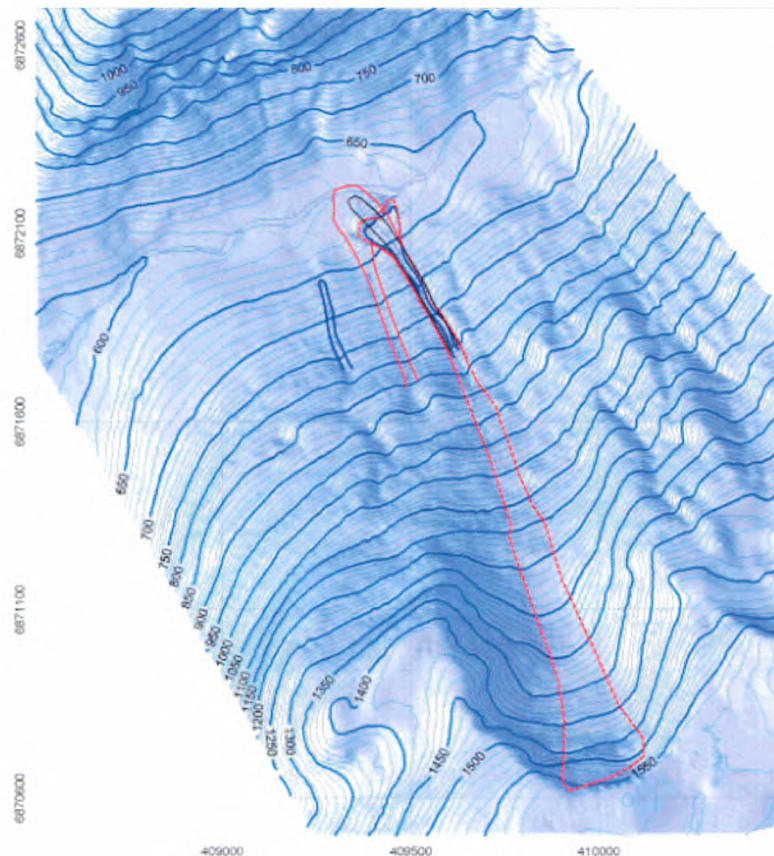


Figure 3.2: Map of the test site with the avalanches recorded in Winter 2003/2004. The dotted red line indicates the artificially released avalanche on 28 February 2004. The other avalanches are represented as follows: black=20031204-20031217, blue=20040204, red solid=20040224-25.



There is limited information about the avalanches during December since they occurred in prolonged storm conditions with bad visibility and continuous avalanche hazard in the runout zone. Concerning the recording of the 4th of December the measurements are somewhat ambiguous. The measurements of the other avalanches also show some unexpected results, something which may be explained by the fact that early season small avalanches sometimes miss one of the load cell sites in the path. Instead the front part of the avalanche may follow the brook depression to the side of the load cell sites. Later in the season this depression is usually filled with snow.

Avalanche 20031204 15:19

Avalanche code (UNESCO/IAHS 1981): A3, B2, C7, D2, E7, F0, G7, H1, J1; unconfirmed.

Weather and avalanche summary At 930 m a.s.l the air temperature was 0.4°C with a 24 hour high of 4.2°C. WSW-wind of 6.3 m s⁻¹ with gusts up to 22 m s⁻¹. Wet snow. No actual observation of the debris.

Results N/A

Avalanche 20031215 16:40

Avalanche code (UNESCO/IAHS 1981): A1, B2, C1, D2, E7, F4, G1, H1, J1.

Weather and avalanche summary Natural, dry small avalanche. At 930 m a.s.l the air temperature was -6.6°C with a 24 hour high of -5.6°C . NNW-wind of 6.3 m s^{-1} with gusts up to 20 m s^{-1} . Heavy snow. No actual observation of the debris.

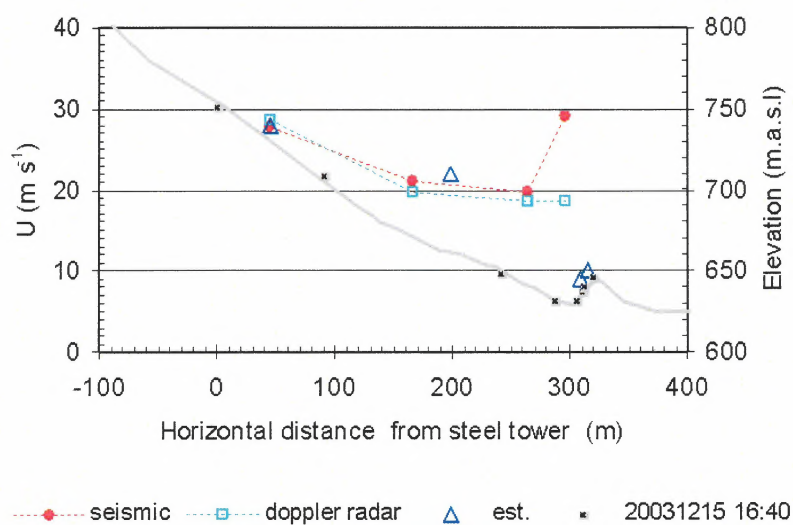
Results

Figure 3.3: *Avalanche 20031215 16:40: Estimated averaged front velocity between various sensors (marked by \boxtimes).*

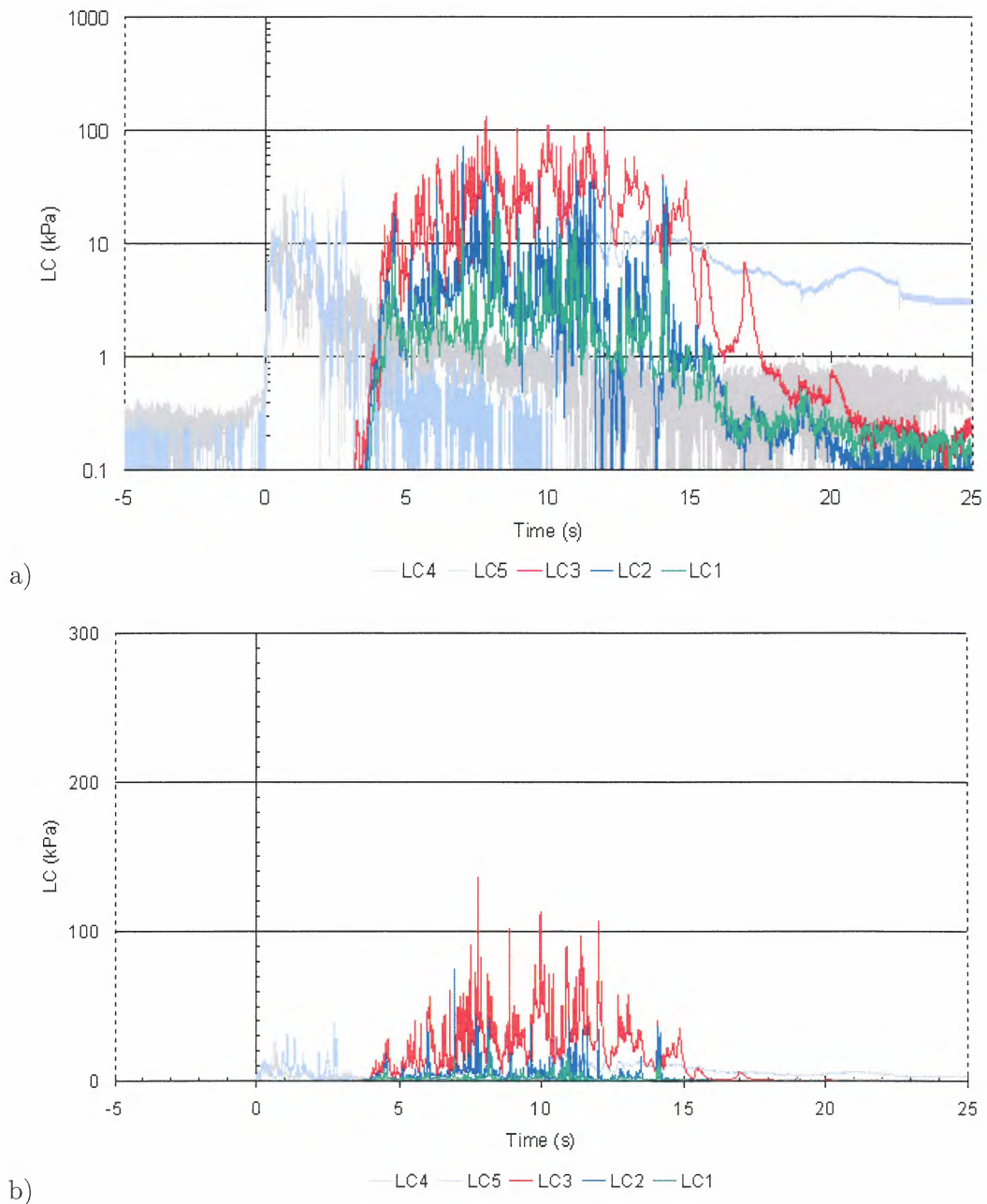


Figure 3.4: Avalanche 20031215 16:40: Load cell measurements: pressure vs time; a) logarithmic and b) linear presentation.

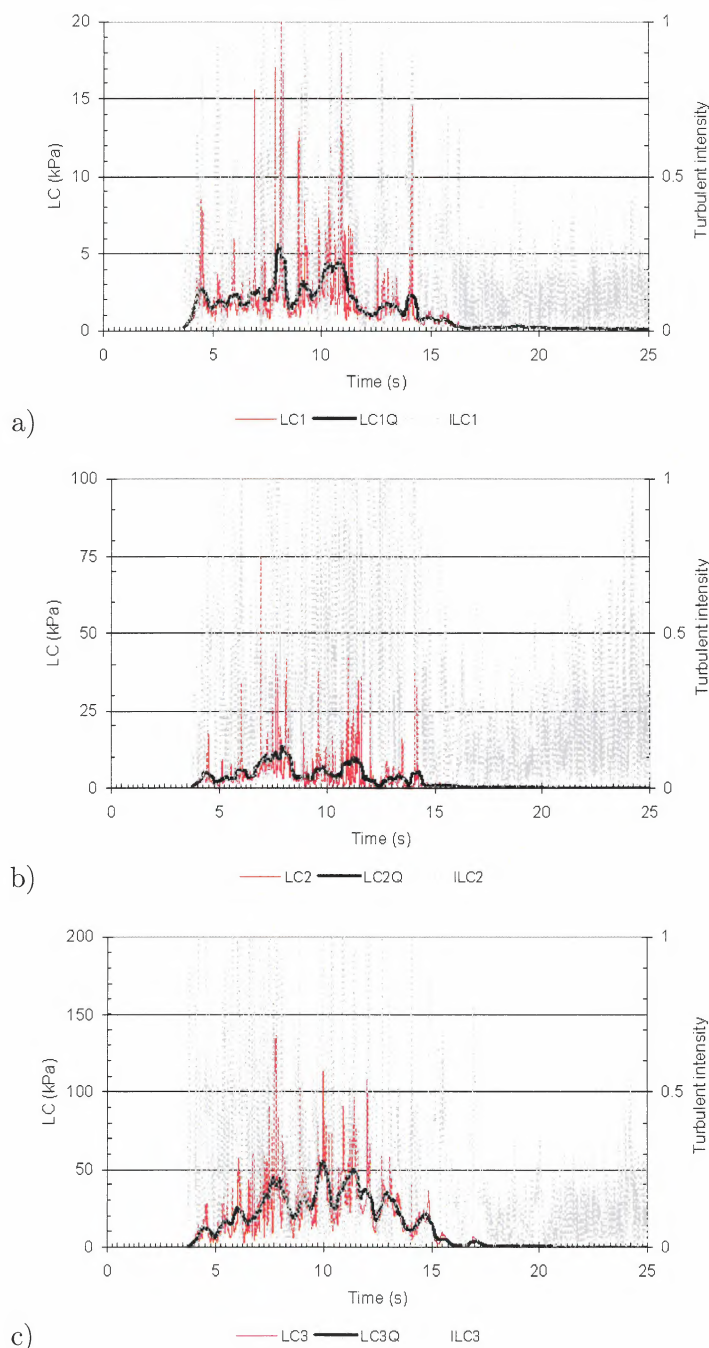


Figure 3.5: *Avalanche 20031215 16:40: Load cell measurements: pressure vs time; shown is the measured value (LCX) and a running mean (LCXQ) taken over 0.5 s (approximately between 5 m to 15 m spatial resolution). In addition, the turbulent intensity is presented (see (Eq. 1.2) for definition). Obvious is the high turbulent intensity indicating a highly fluidized avalanche. a) LC1, b) LC2, and c) LC3.*

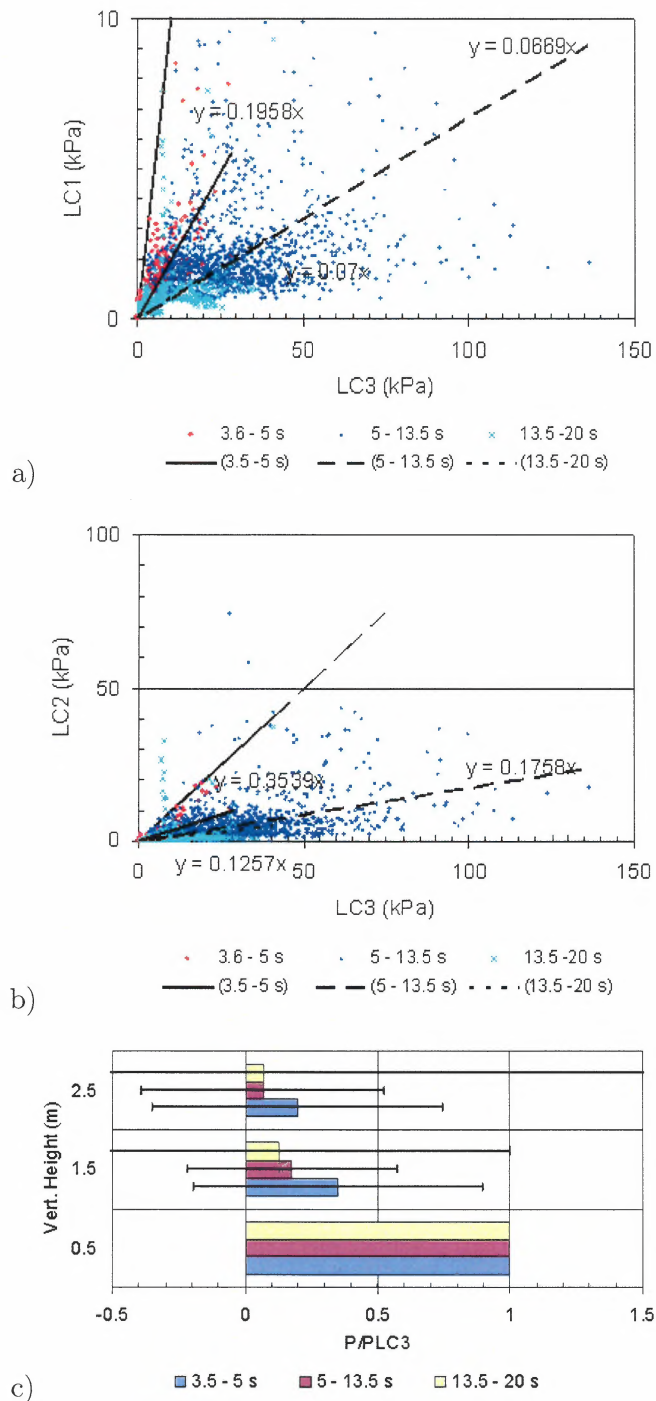


Figure 3.6: Avalanche 20031215 16:40: a) and b) show a plot of LC1 and LC2 vs LC3, respectively, and linear trends for different periods. c) presents a normalized pressure profile for the different periods. Assuming a negligible vertical velocity gradient, the profile is an indication of the density profile within the avalanche. However some care has to be taken as the ration A_a/A_m is not known. The error bars mark the relative error from the linear relation $(LC_X - a LC_3)/(a LC_3)$, here a is the slope of the linear interpolation. High errors indicate also high fluctuations.

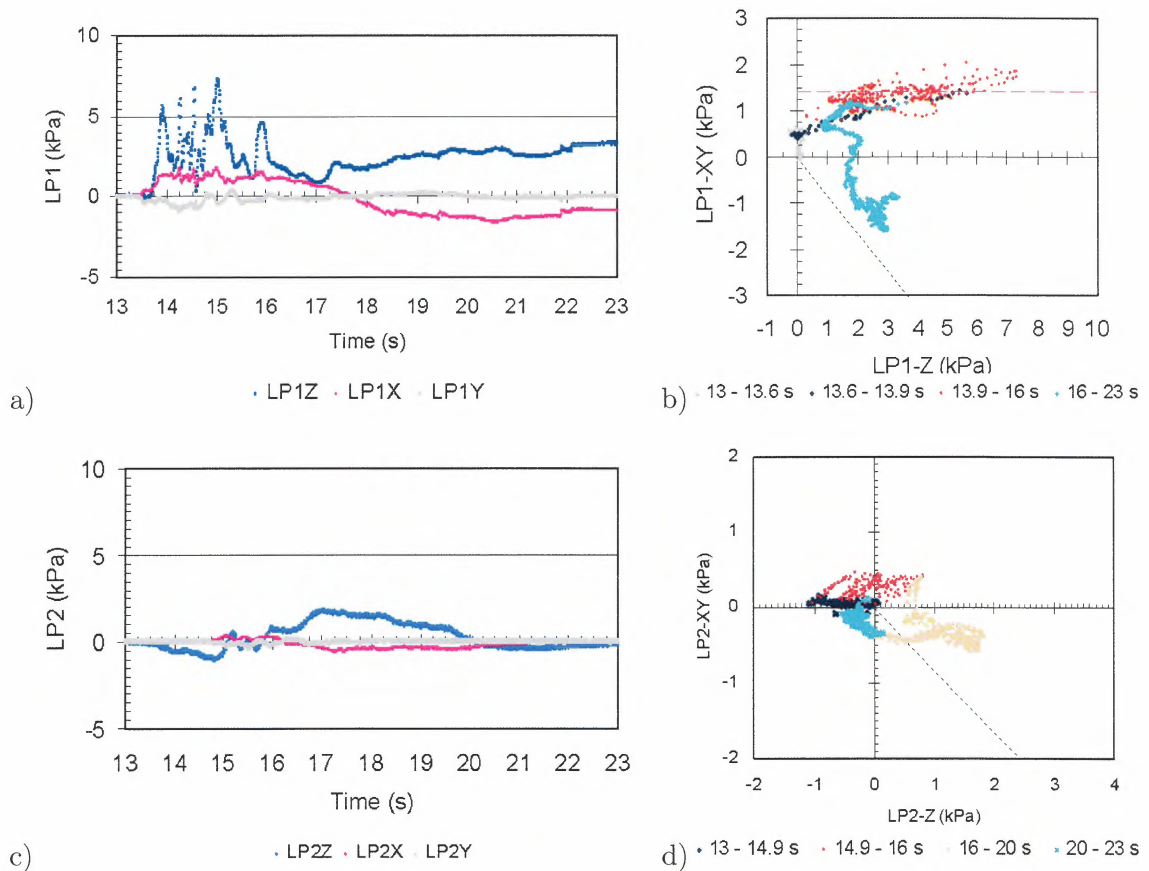


Figure 3.7: Avalanche 20031215 16:40: Load plate measurements: a) LP1 vs time; b) LP1-XY vs LP1-Z; c) LP2 vs time; d) LP2-XY vs LP2-Z; here LP*-XY is the total shear stress and the sign indicates its direction parallel to the x-axis (see Fig. 1.1). Obvious is a relatively high negative normal force on LP2Z without simultaneous shear stress for which an explanation is still lacking. A small negative normal stress is also seen in a) just before the avalanche hits the plate.



Avalanche 20031217 03:24

Avalanche code (UNESCO/IAHS 1981): A1, B2, C1, D2, E7, F4, G7, H1, J1.

Weather and avalanche summary Natural, dry small avalanche. At 930 m a.s.l the air temperature was 0.9°C, with temperatures below 0°C the preceding 24 hours. SW-wind of 2.2 m s⁻¹ with gusts up to 9 m s⁻¹. Heavy snow turning to rain in the lower altitudes.

Results This avalanche allowed an estimate of the velocity distribution within the avalanche at the concrete structure (see for example 3.12). The estimate is based on a correlation between pressure measurements (their structure) at the steel tower and at the concrete wedge. In this way it was possible to determine the front velocity and a velocity in the rear part of the avalanche. Finally, a linear decrease of the velocity between the to points in the avalanche was assumed.

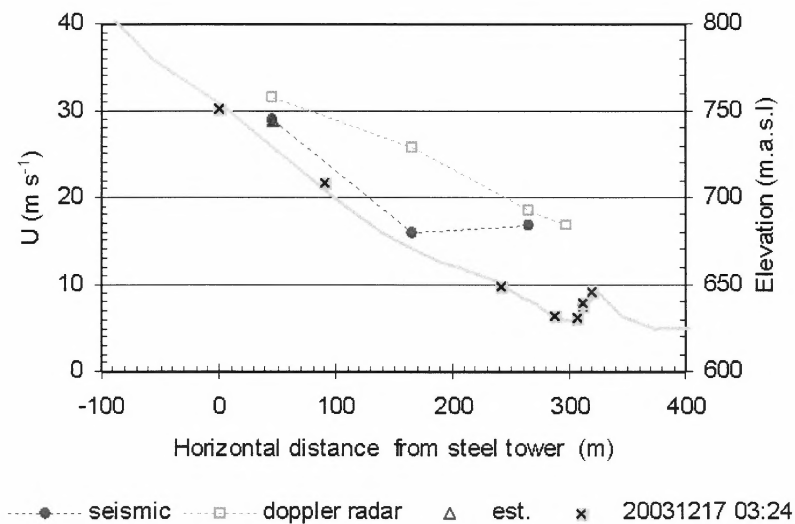


Figure 3.8: *Avalanche 20031217 03:24: Estimated averaged front velocity between various sensors (marked by □).*

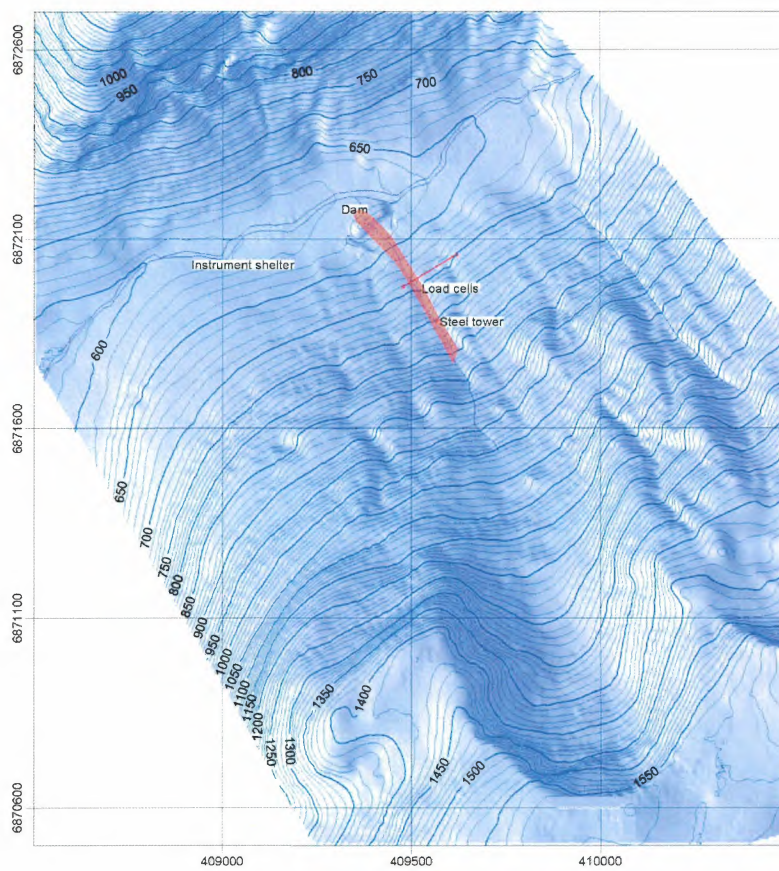


Figure 3.9: Avalanche 20031217 03:24: Deposition map combining the avalanches 20031215 16:40 and 20031217 03:24

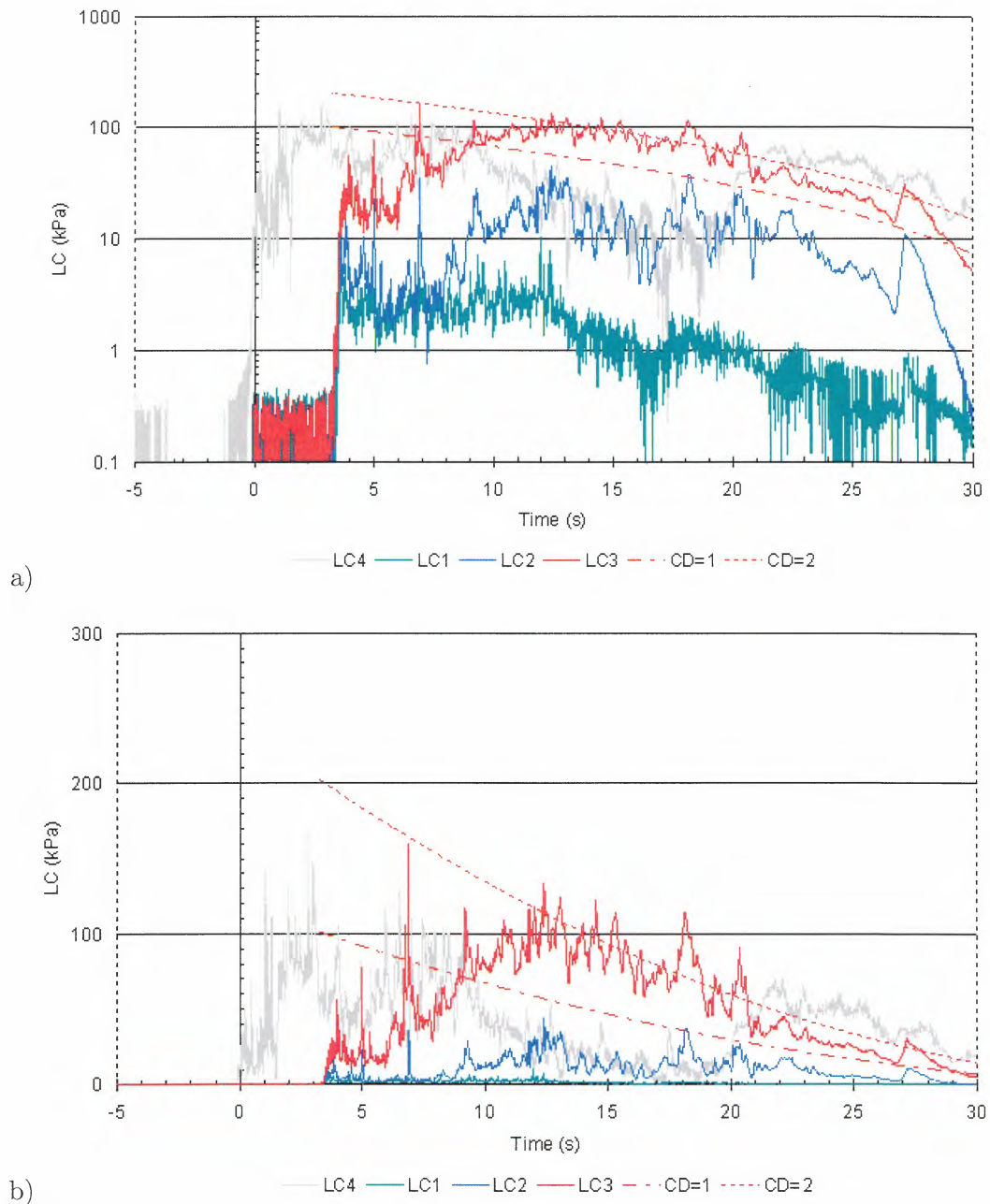


Figure 3.10: Avalanche 20031217 03:24: Load cell measurements: pressure vs time. Added are calculated pressure curves with $\rho_0 = 300 \text{ kg m}^{-3}$ and $C_D=1$ and $C_D=2$ and estimated speed. a) logarithmic and b) linear presentation.

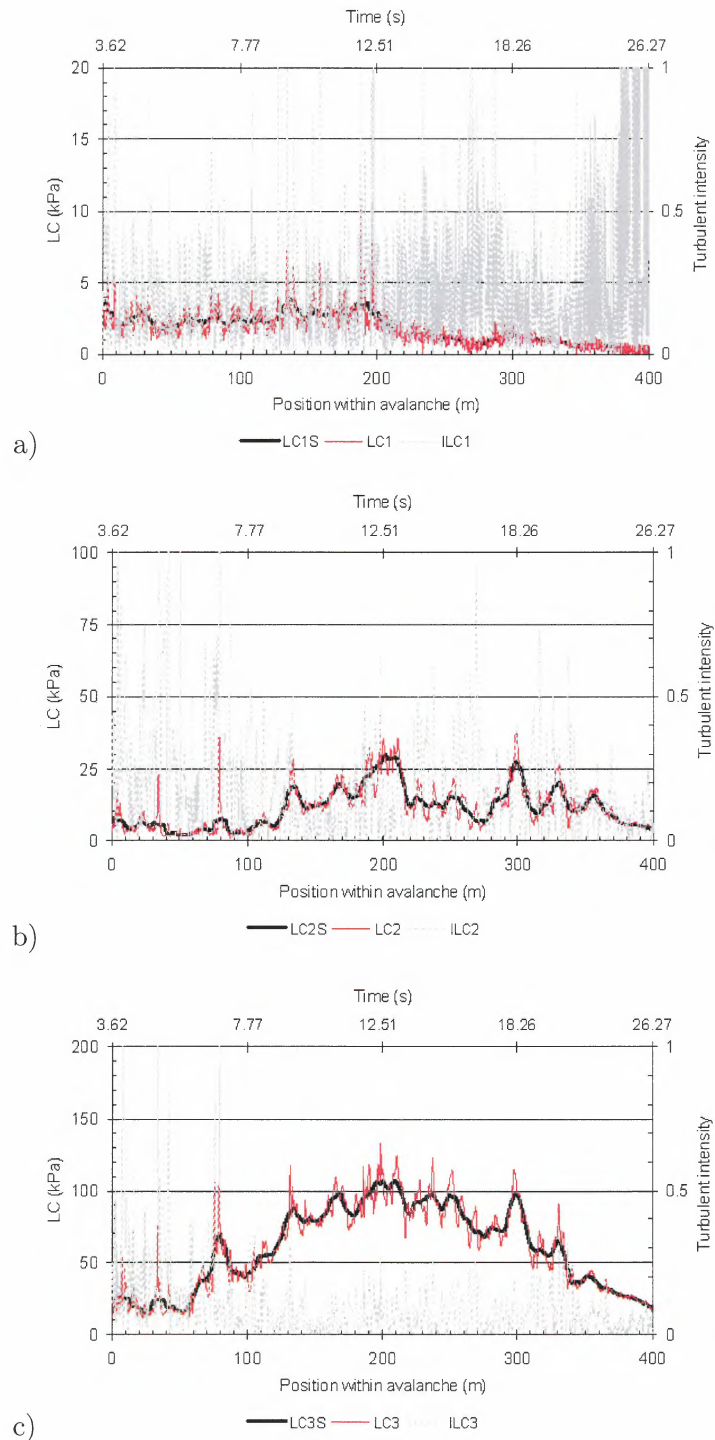


Figure 3.11: *Avalanche 20031217 03:24: Load cell measurements: pressure vs time; shown is the measured value (LCX) and a running mean taken over 5 m (LCXS). In addition, the turbulent intensity is presented (see (Eq. 1.2) for definition). Obvious is the high turbulent intensity at the front of the avalanche and in the upper part indicating a highly fluidized layer. a) LC1, b) LC2, and c) LC3.*

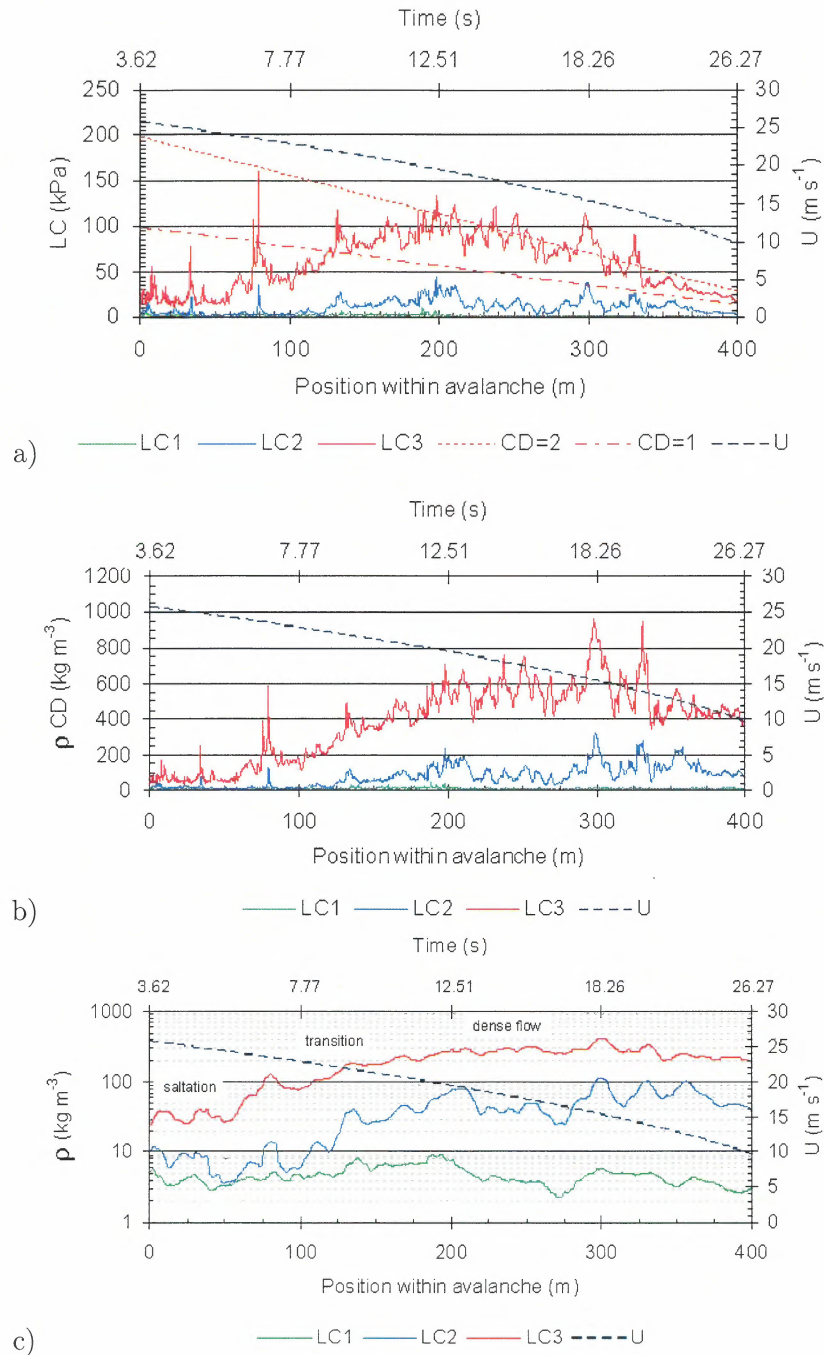


Figure 3.12: Avalanche 20031217 03:24: Load cell measurements; a) pressure vs position within avalanche. Added are also calculated pressure curves with $\rho_0 = 300 \text{ kg m}^{-3}$ and $C_D = 1$ and $C_D = 2$. b) ρC_D vs position within avalanche; c) ρ vs position within avalanche assuming $C_D = 2$, pressure data base on a running mean taken over 5 m. In addition, the estimated velocity, U , is shown.

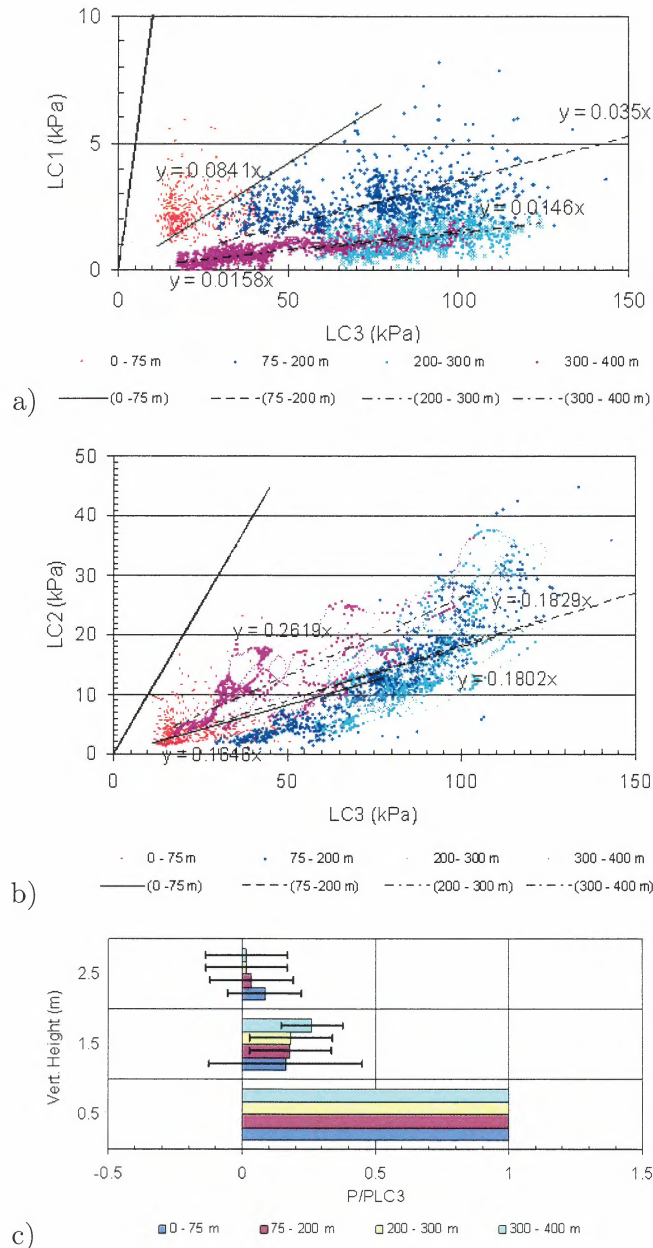


Figure 3.13: Avalanche 20031217 03:24: a) and b) show a plot of LC1 and LC2 vs LC3, respectively, and linear trends for different spatial intervals. c) presents a normalized pressure profile for the different spatial intervals. Assuming a negligible vertical velocity gradient, the profile is an indication of the density profile within the avalanche. However some care has to be taken as the ration A_a/A_m is not known. This is especially the case for the upper load cell. The error bars mark the relative error from the linear relation $(LC_X - a LC_3)/(a LC_3)$, here a is the slope of the linear interpolation. High errors would indicate also high fluctuations.



Avalanche 20040204 06:10

Avalanche code (UNESCO/IAHS 1981): A1, B2, C7, D2, E7, F3, G2, H4, J1.

Weather and avalanche summary A natural wet snow avalanche ran during rain and mild weather conditions in the lower avalanche path. The temperature at the instrument shelter was 9.9°C at the evening before (19:00 h) and the 0°C isotherm was clearly above the starting zone. However, the exact elevation of the starting zone could not be determined initially because of bad visibility. Estimated volume in the runout zone is around 50000 m³.

At 930 m a.s.l the air temperature was 0.4°C, with high temperatures of 7.4°C the preceding 24 hours. S-wind of 5.4 m s⁻¹, with gusts up to 19 m s⁻¹. Rain turning to snow.

Snow on the ground in the runout area:

Depth	W	F	K	Size (mm)	G (kg m ⁻³)	Avalanche deposit density from samples of clods (kg m ⁻³)
0	wet	○ 6	1	1	340	
-30	wet	□ 4-6	1	2	350	550
-50	wet	□ 4-6	1	2	440	500

Results This avalanche allowed an estimate of the velocity distribution within the avalanche at the concrete structure (see for example 3.18). The estimate is based on a correlation between pressure measurements (their structure) at the steel tower and at the concrete wedge. In this way it was possible to determine the front velocity and a velocity in the rear part of the avalanche. Finally, a linear decrease of the velocity between the to points in the avalanche was assumed.

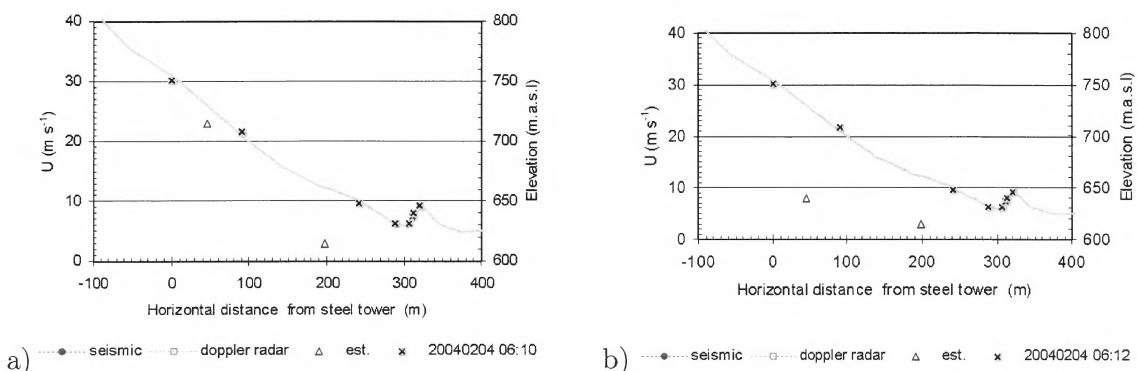


Figure 3.14: Avalanche 20040204 06:10: Estimated averaged front velocity between various sensors (marked by \boxtimes).

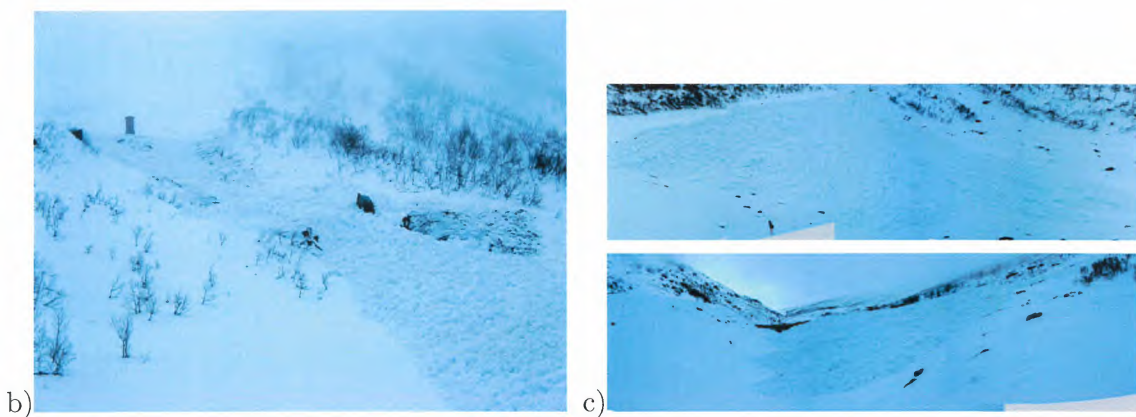
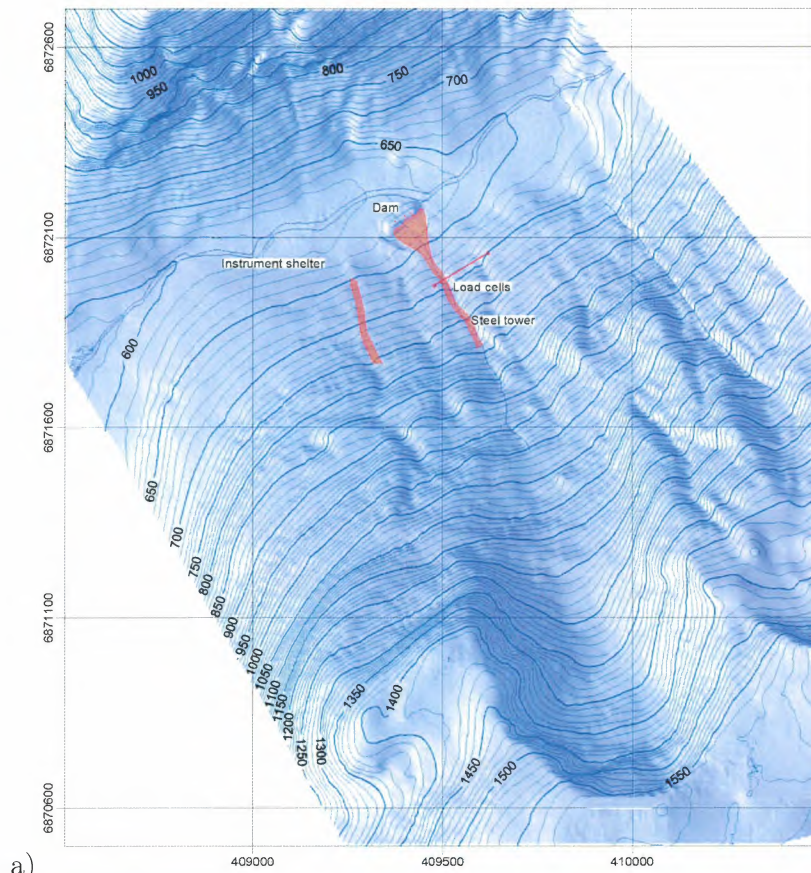


Figure 3.15: *Avalanche 20040204 06:10: Deposition map (upper panel); steel tower and concrete wedge with load cells in the avalanche debris (left photo); view from the dam on deposit (upper right photo) and a side view (lower right photo).*

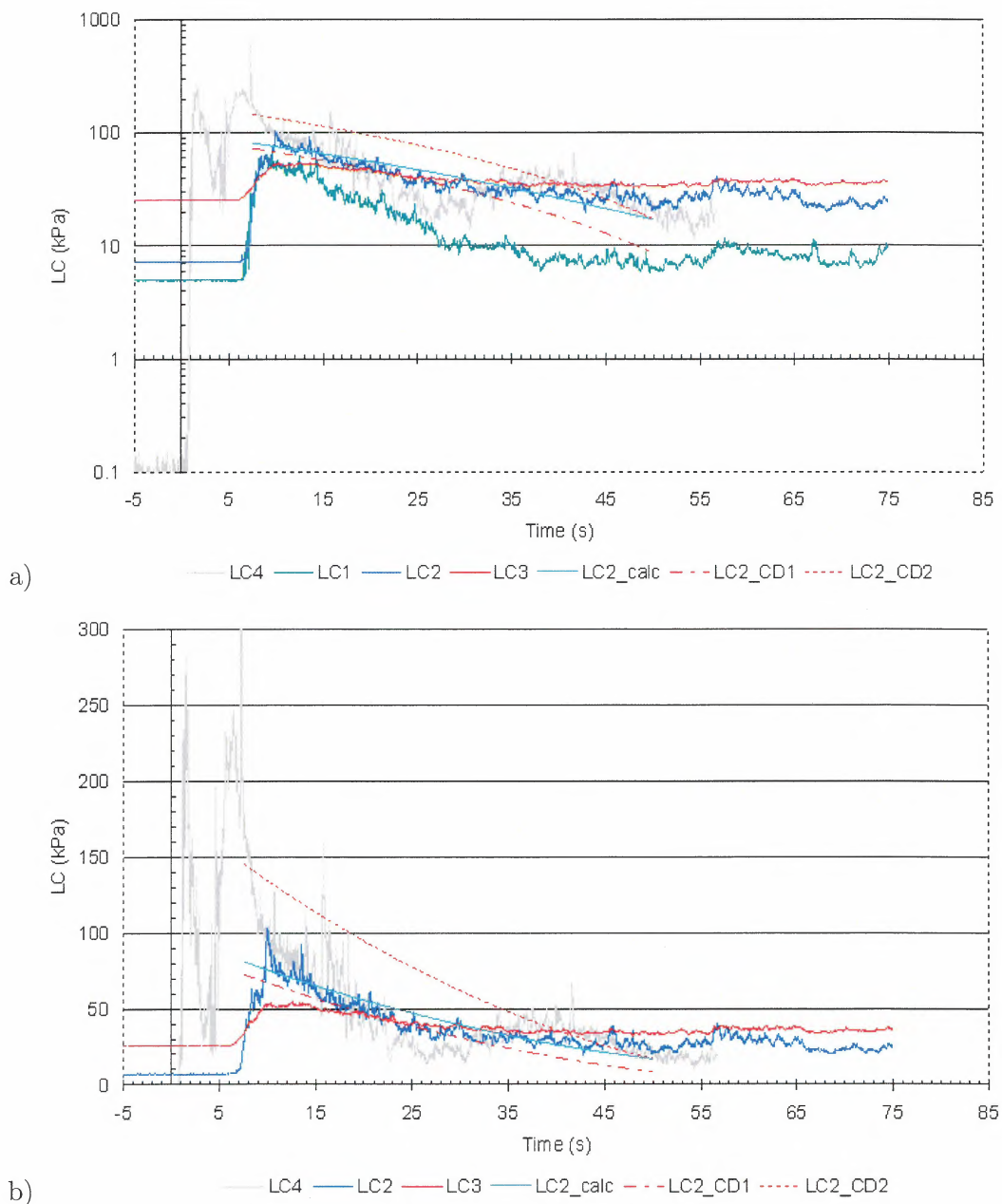


Figure 3.16: *Avalanche 20040204 06:10: Load cell measurements: pressure vs time. Added are calculated pressure curves with $\rho_0 = 300 \text{ kg m}^{-3}$ and $C_D=1$ and $C_D=2$, and $C_D = f(R_e)$. a) logarithmic and b) linear presentation.*

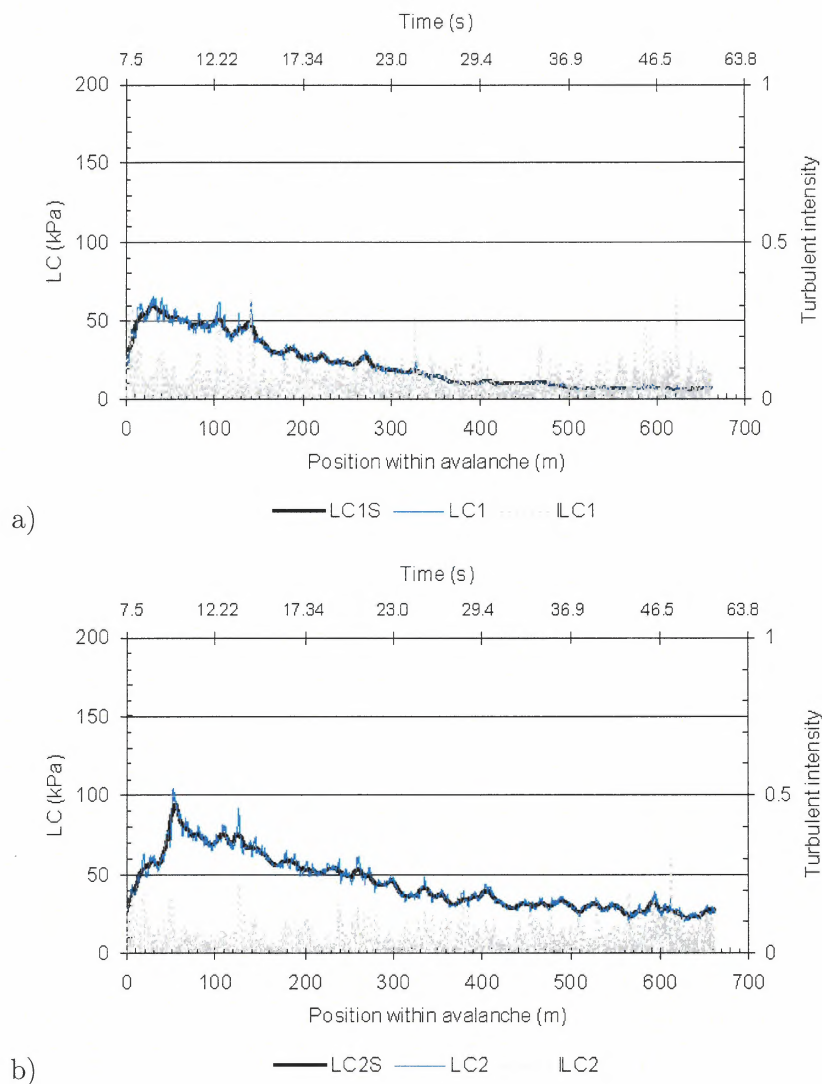


Figure 3.17: *Avalanche 20040204 06:10: Load cell measurements: pressure vs time; shown is the measured value (LCX) and a running mean taken over 5 m (LCXS). In addition, the turbulent intensity is presented (see Eq. (1.2) for definition) The low turbulent intensity indicates a more dense flow regime. a) LC1 and b) LC2. The lower pressure values for LC1 are probably influenced by the flow height not reaching the full sensor height ($A_a < A_m$).*

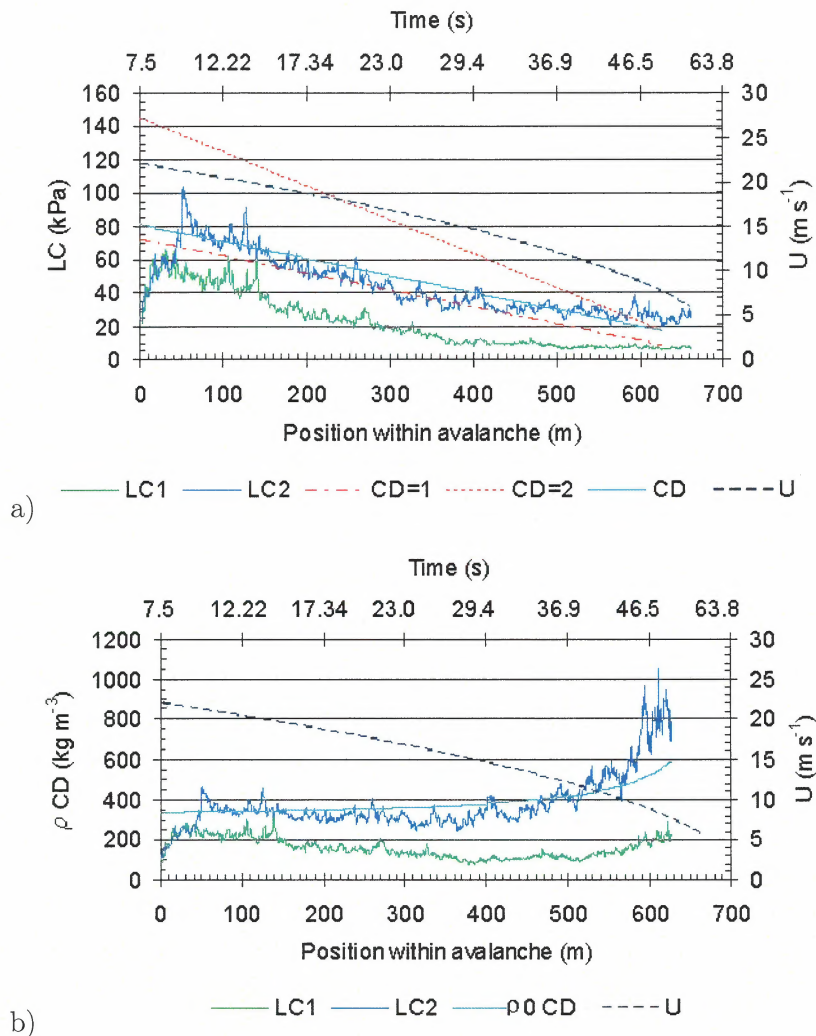


Figure 3.18: Avalanche 20040204 06:10: Load cell measurements: a) pressure vs position within avalanche. Added are also calculated pressure curves with $\rho_0 = 300 \text{ kg m}^{-3}$ and $C_D = 1$, $C_D = 2$, and $C_D = f(R_e)$ (see Fig 1.2, $\tau_c = 700 \text{ Pa}$). b) ρC_D vs position within avalanche. For comparison, the calculated curve with $\rho_0 = 300 \text{ kg m}^{-3}$ and $C_D = f(R_e)$ is also presented. In addition, the estimated velocity, U , is shown.

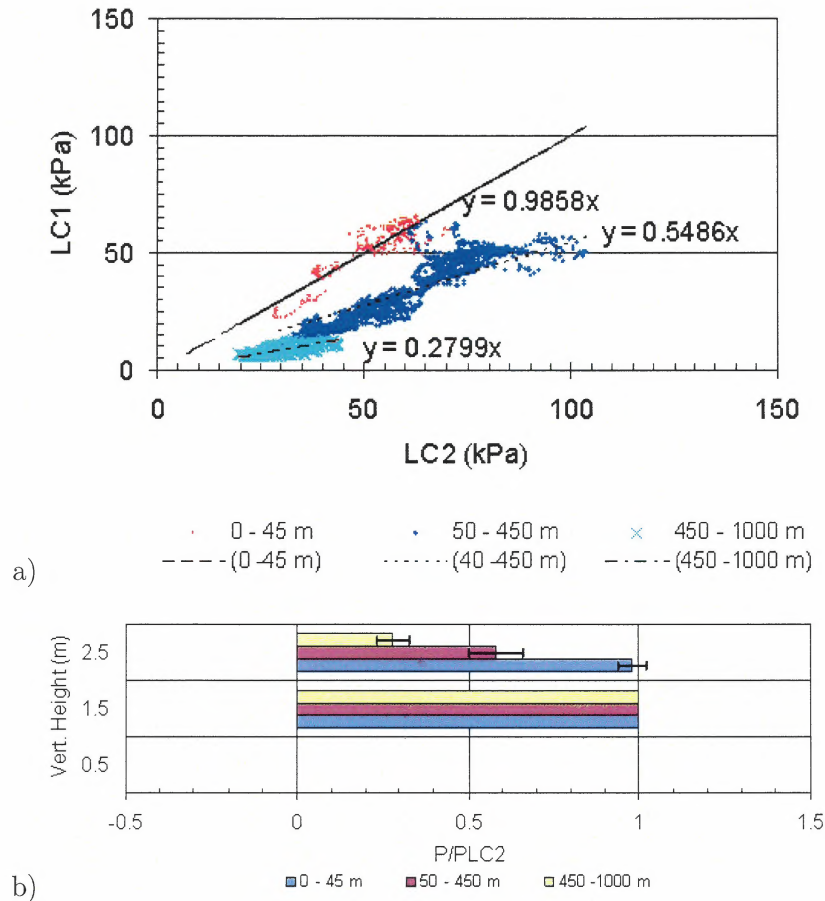


Figure 3.19: *Avalanche 20040204 06:10: a) and b) show a plot of LC1 vs LC2 and linear trends for different periods. b) presents a normalized pressure profile for the different periods. Assuming a negligible vertical velocity gradient, the profile is an indication of the density profile within the avalanche. However some care has to be taken as the ration A_a/A_m is not known. This is especially the case for the upper load cell. The error bars mark the relative error from the linear relation $(LC_X - a LC_2)/(a LC_2)$, here a is the slope of the linear interpolation. The low errors would indicate also low fluctuations.*

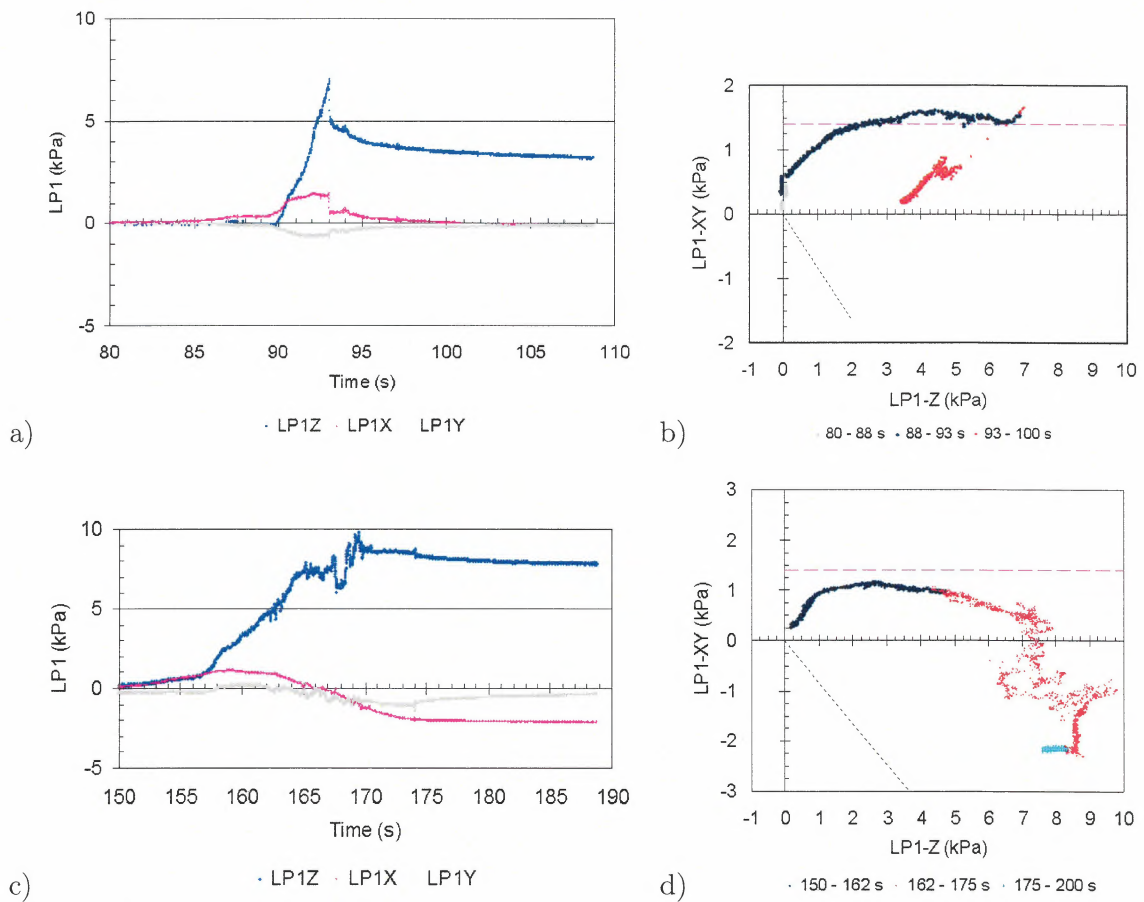


Figure 3.20: *Avalanche 20040204 06:10: Load plate measurements; a) LP1 vs time; b) LP1-XY vs LP1-Z; c) LP1 vs time; d) LP1-XY vs LP1-Z; here LP1-XY is the total shear stress and the sign indicates its direction parallel to the x-axis (see Fig. 1.1).*

Three separate relatively small avalanches ran in the course of less than 24 hours. Because of the weather conditions with continuous snow and wind it was impossible to discern the debris of the individual avalanches. All of the avalanches probably released as dry snow avalanches.

Avalanche 20040224 08:50

Avalanche code (UNESCO/IAHS 1981): A1, B2, C1, D2, E7, F4, G1, H1, J1.

Weather and avalanche summary At 930 m a.s.l the air temperatures were between -6.1 and -4°C . Strong easterly wind of 9 m s^{-1} , with gusts up to 20 m s^{-1} . Snow and drifting snow.

Results

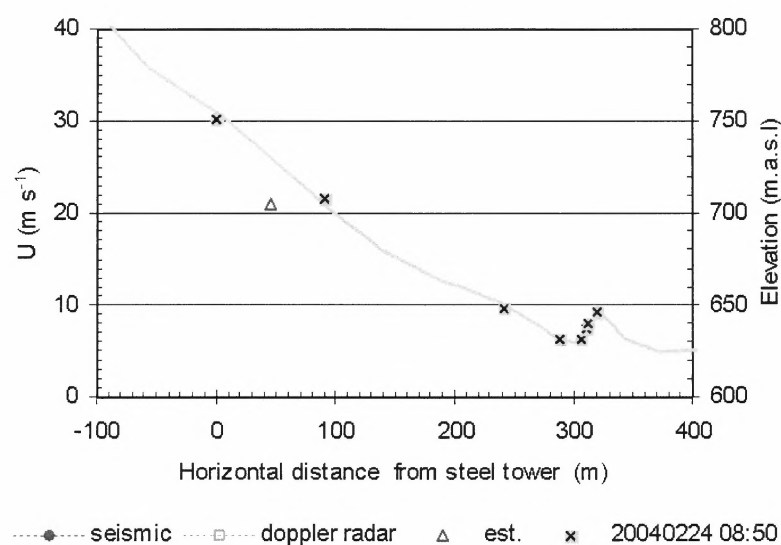


Figure 3.21: *Avalanche 20040224 08:50: Estimated averaged front velocity between various sensors (marked by \boxtimes).*

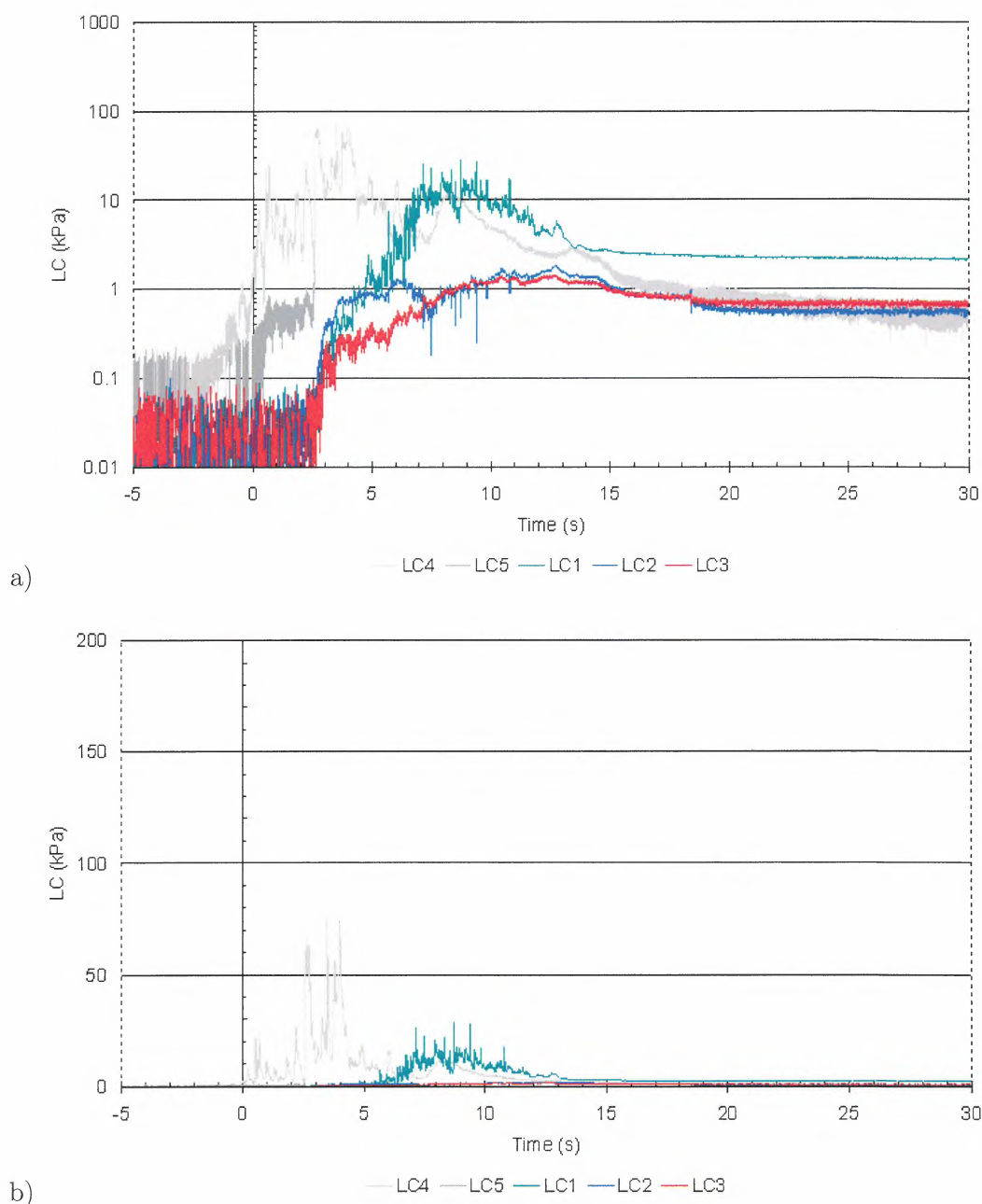


Figure 3.22: *Avalanche 20040224 08:50: Load cell measurements: pressure vs time; a) logarithmic and b) linear presentation. At this time, probably all load cell except maybe LC4 were partly or totally buried. Presented values are all reduced by an offset. Thus, the shown values for LC2, LC3 and also LC1 are basically forces transmitted through the snowpack during the avalanche passage. Offset: LC1 = 5.9 kPa, LC2 = 51.2 kPa, LC3 = 61.2 kPa.*



Avalanche 20040224 22:30

Avalanche code (UNESCO/IAHS 1981): A1, B2, C1, D2, E7, F4, G1, H1, J1.

Weather and avalanche summary At 930 m a.s.l the air temperatures were between -6.1 and -4°C. Strong easterly wind of 9 m s⁻¹, with gusts up to 20 m s⁻¹. Snow and drifting snow.

Results

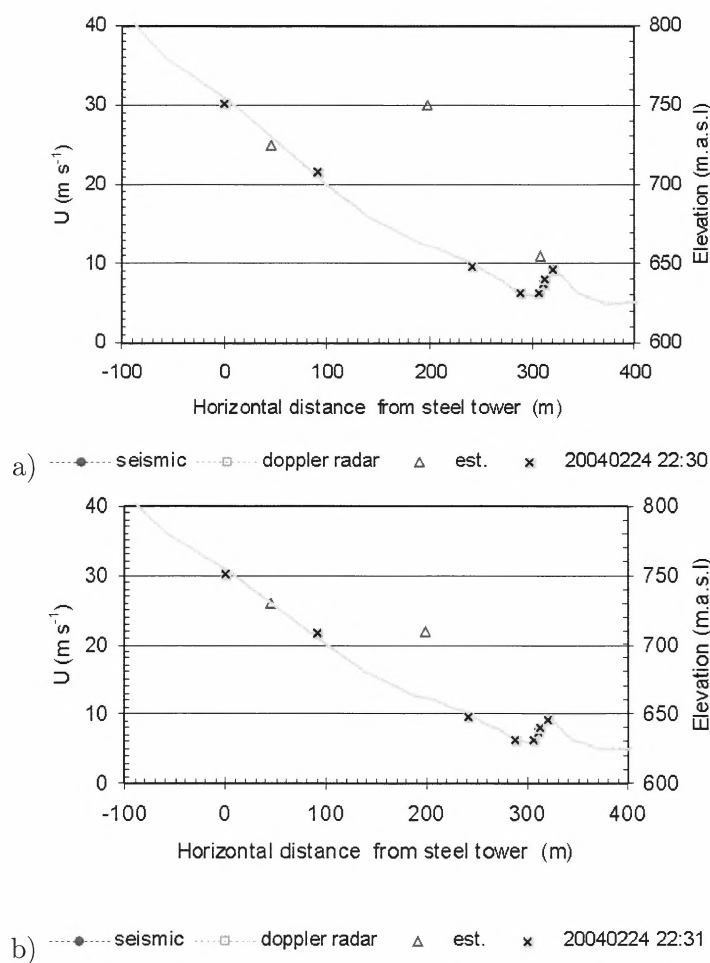


Figure 3.23: *Avalanche 20040224 22:30: Estimated averaged front velocity between various sensors (marked by ☒).*

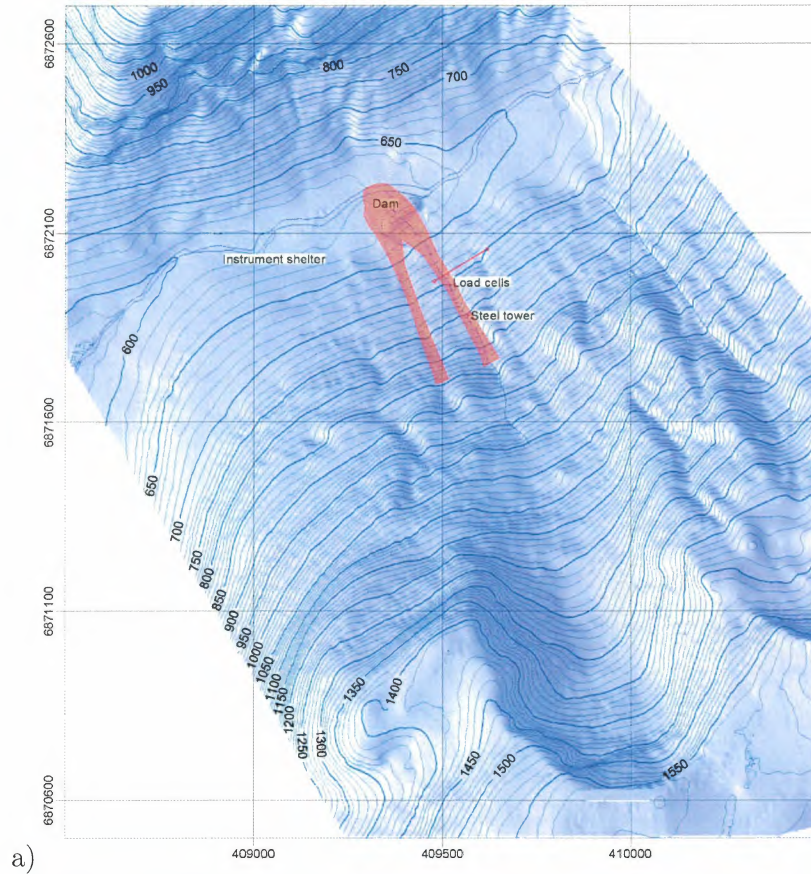


Figure 3.24: Deposition map combining the avalanches from 20020224 and 20040225 (upper panel); side view of the dam with slightly visible traces of avalanche debris (photo).

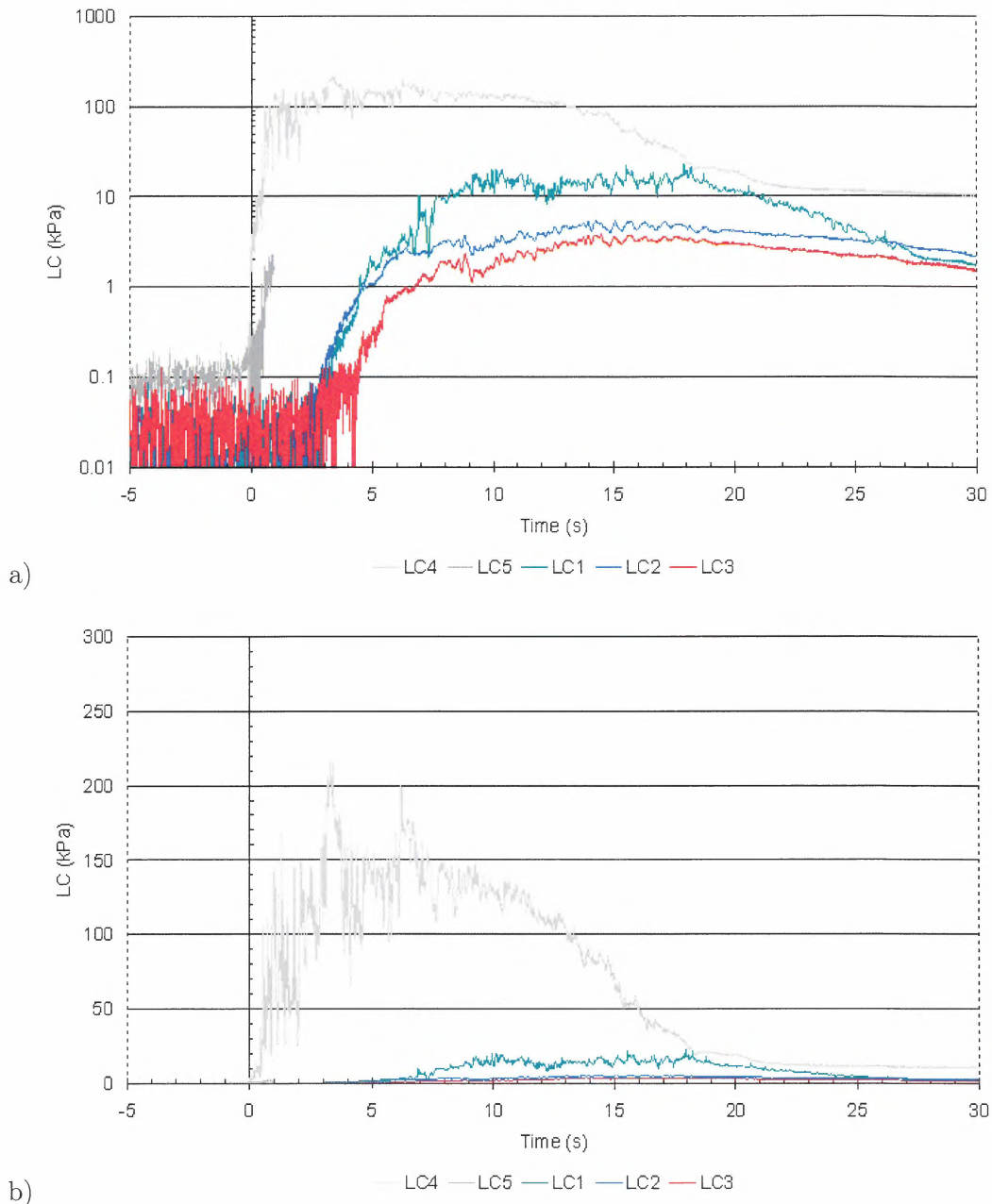


Figure 3.25: *Avalanche 20040224 22:30: Load cell measurements: pressure vs time; a) logarithmic and b) linear presentation. At this time, probably all load cell except maybe LC4 were partly or totally buried. Presented values are all reduced by an offset. Thus, the shown values for LC2, LC3 and also LC1 are basically forces transmitted through the snowpack during the avalanche passage. Offset: LC1 = 7.5 kPa, LC2 = 53.4 kPa, LC3 = 64.5 kPa.*

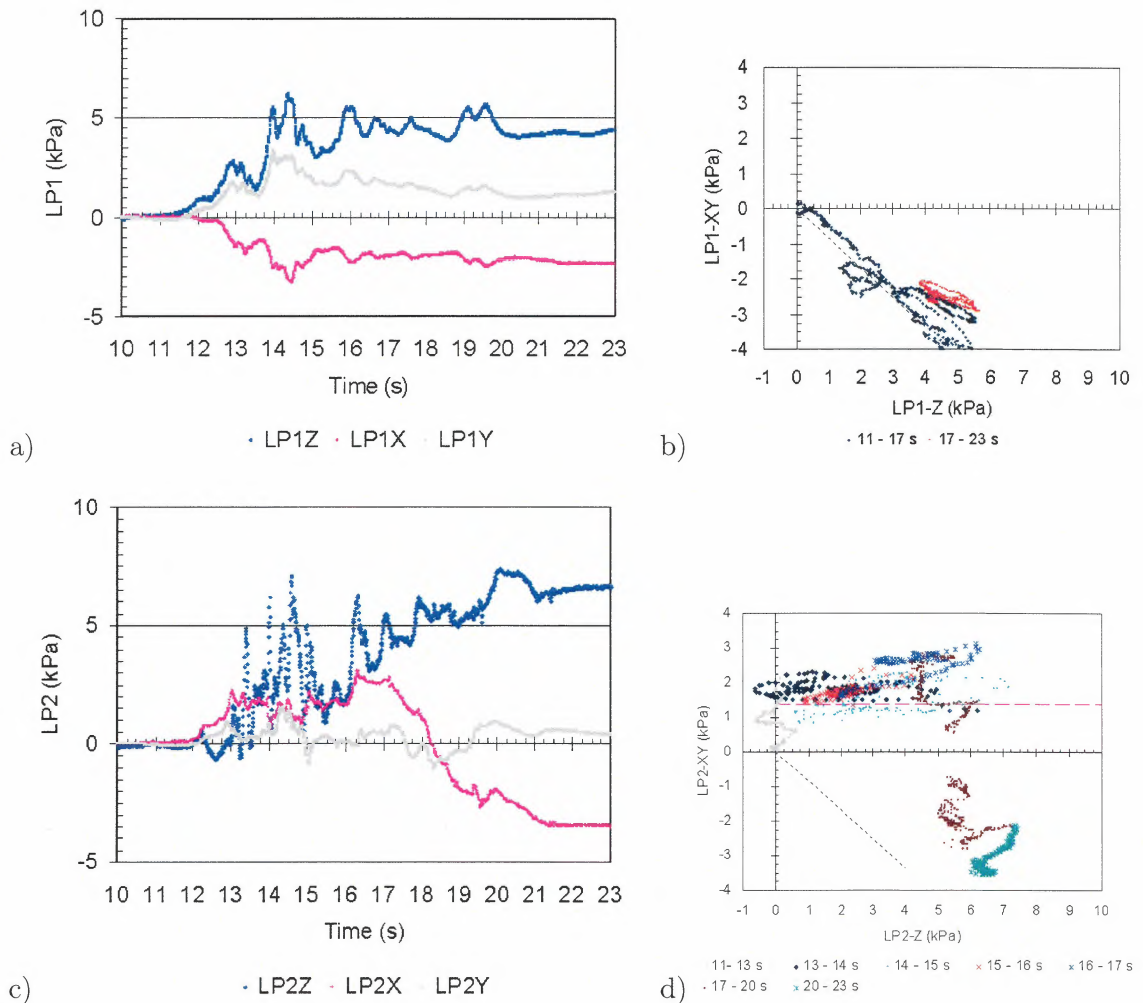


Figure 3.26: Avalanche 20040224 22:30: Load plate measurements: a) LP1 vs time; b) LP1-XY vs LP1-Z; c) LP2 vs time; d) LP2-XY vs LP2-Z; here LP*-XY is the total shear stress and the sign indicates its direction parallel to the x-axis (see Fig. 1.1).

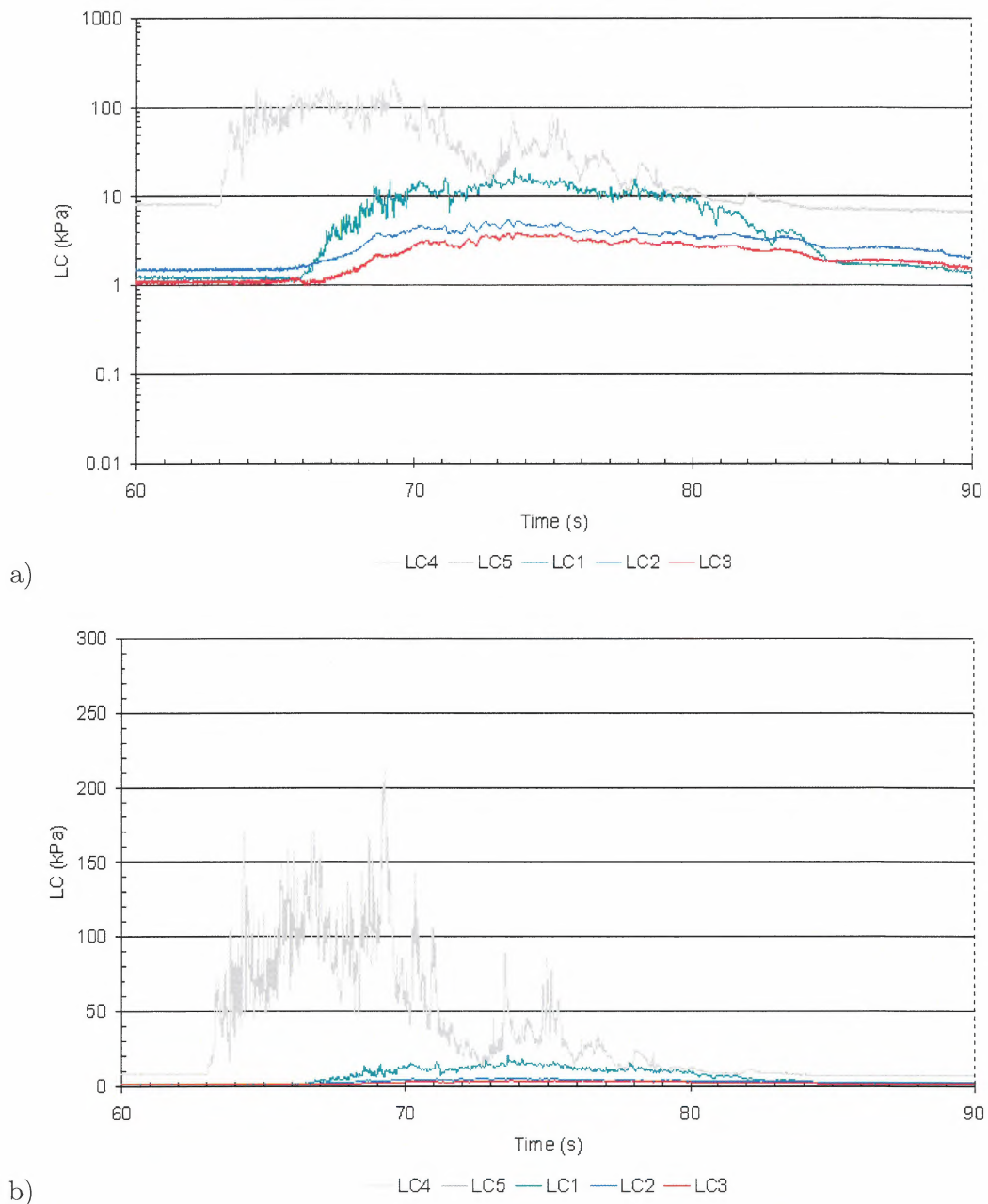


Figure 3.27: *Avalanche 20040224 22:31: Load cell measurements: pressure vs time; a) logarithmic and b) linear presentation. At this time, probably all load cell except maybe LC4 were partly or totally buried. Presented values are all reduced by an offset. Thus, the shown values for LC2, LC3 and also LC1 are basically forces transmitted through the snowpack during the avalanche passage. Offset: LC1 = 7.5 kPa, LC2 = 53.4 kPa, LC3 = 64.5 kPa.*

Avalanche 20040228 15:30

Avalanche code (UNESCO/IAHS 1981): A1, B2, C1, D2, E7, F4, G2, H1, J4.

Weather and avalanche summary On February 28th, a dry snow avalanche was released by detonating explosives in the starting zone. The resulting mixed snow avalanche ran the length of the path. Although much of the debris was retained by the dam, the dust cloud went far beyond. The volume of the deposit in the run-out zone below the load cells on the concrete structure is estimated to around 100,000 m³.

The avalanche was triggered in fair weather. At 930 m a.s.l the air temperature was around -12°C, which was also the highest temperature during the preceding 24 hours. NS-wind of 5.4 m s⁻¹, with gusts up to 9 m s⁻¹. Clear weather and partly sunshine.

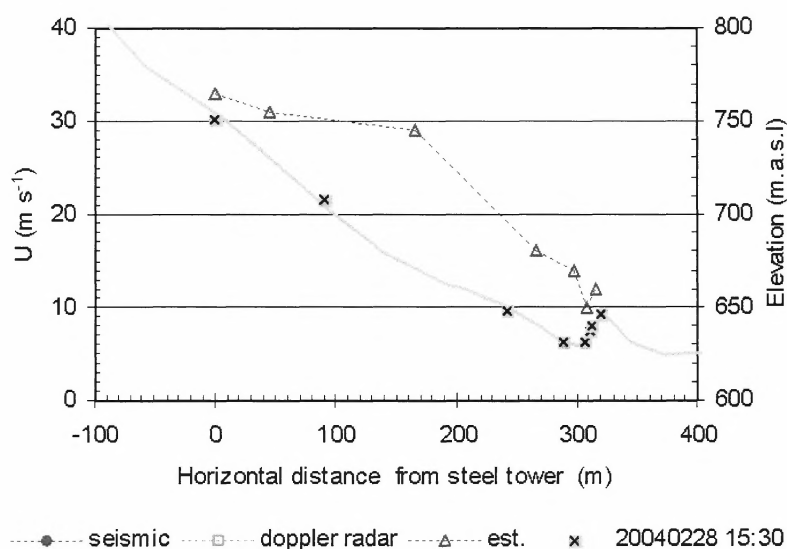
Results

Figure 3.28: *Avalanche 20040228 15:30: Estimated averaged front velocity between various sensors (marked by ☒).*

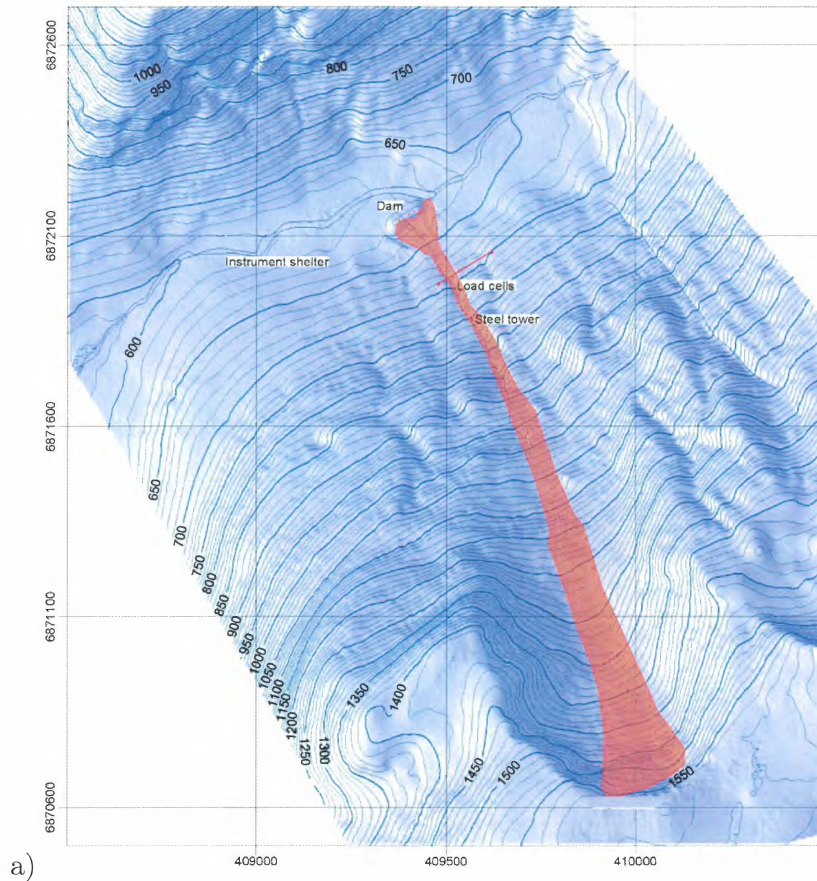


Figure 3.29: Avalanche 20040228 15:30: Deposition/outline map (upper panel); area of the dam before (left right photo) and after (right photo) the avalanche. The hand cloth in the inset indicates the size of the clods.

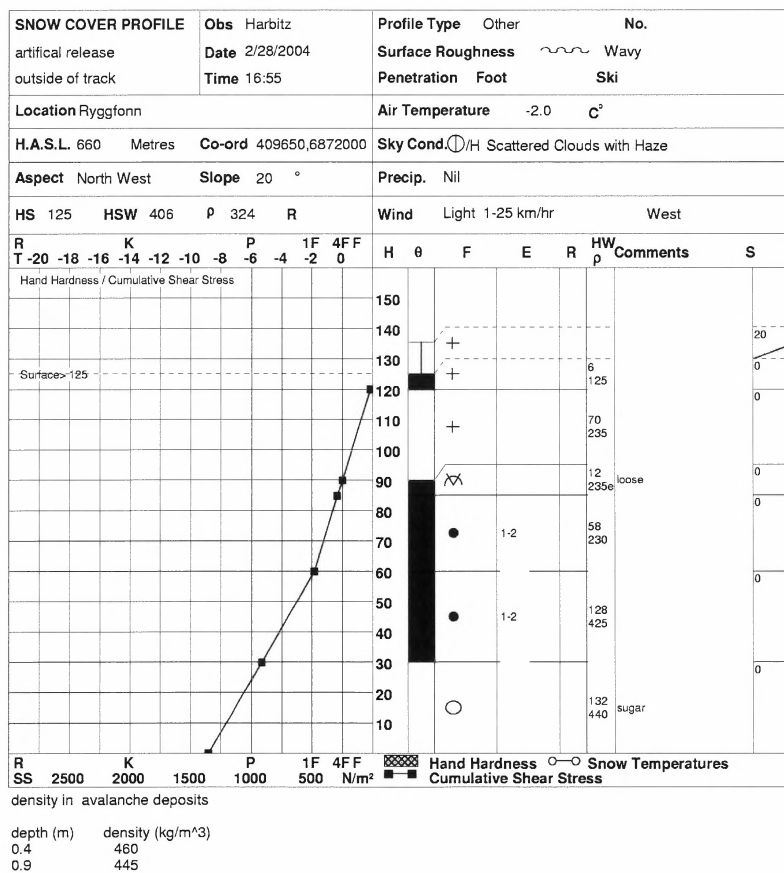


Figure 3.30: Avalanche 20040228 15:30: snow profile aside of the track

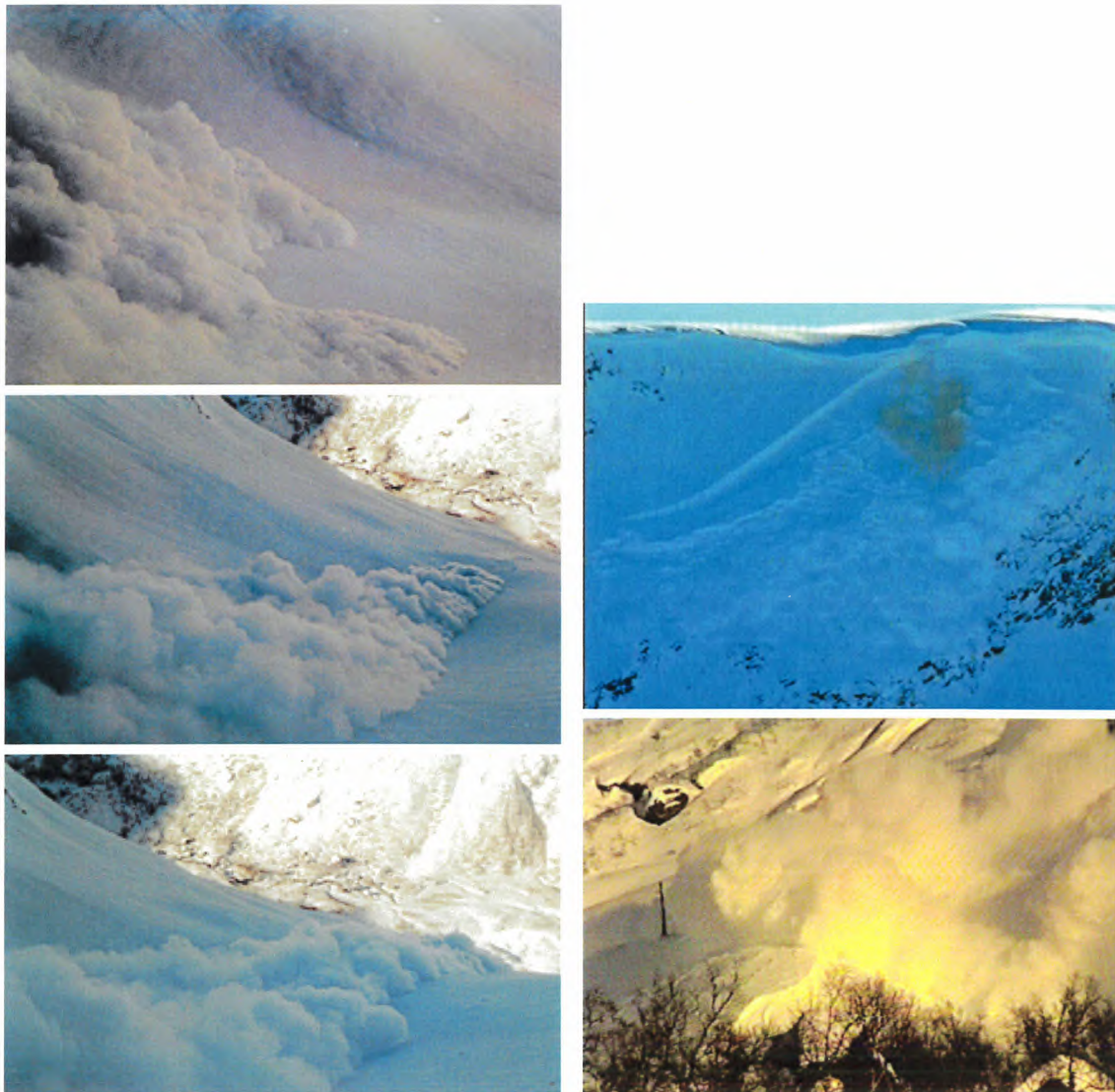


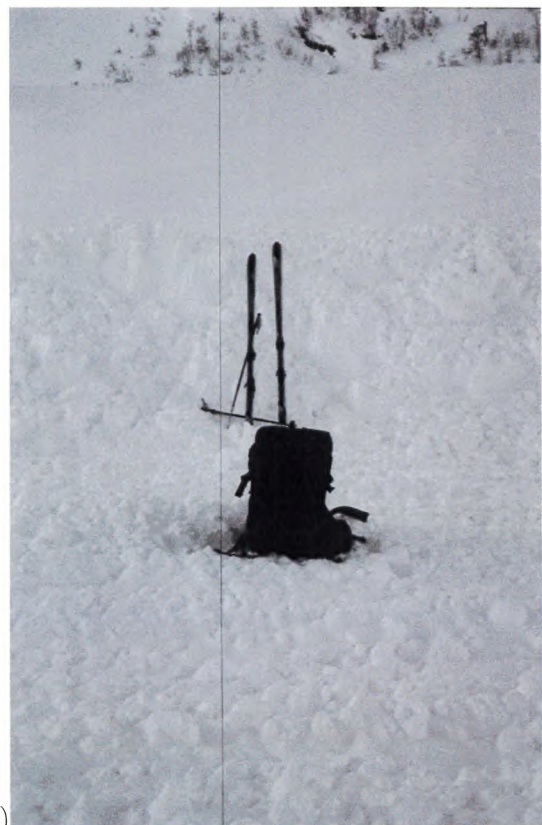
Figure 3.31: Avalanche 20040228 15:30: Avalanche snap shots; track (left panel); release area (upper right panel); impact on dam (lower right panel)



a)



b)



c)

Figure 3.32: *Avalanche 20040228 15:30: Deposition pattern; a) concrete wedge; b) view along the track; c) deposition before the dam (see also Fig. 3.29 c); photo shows the wave on the right hand side there).*

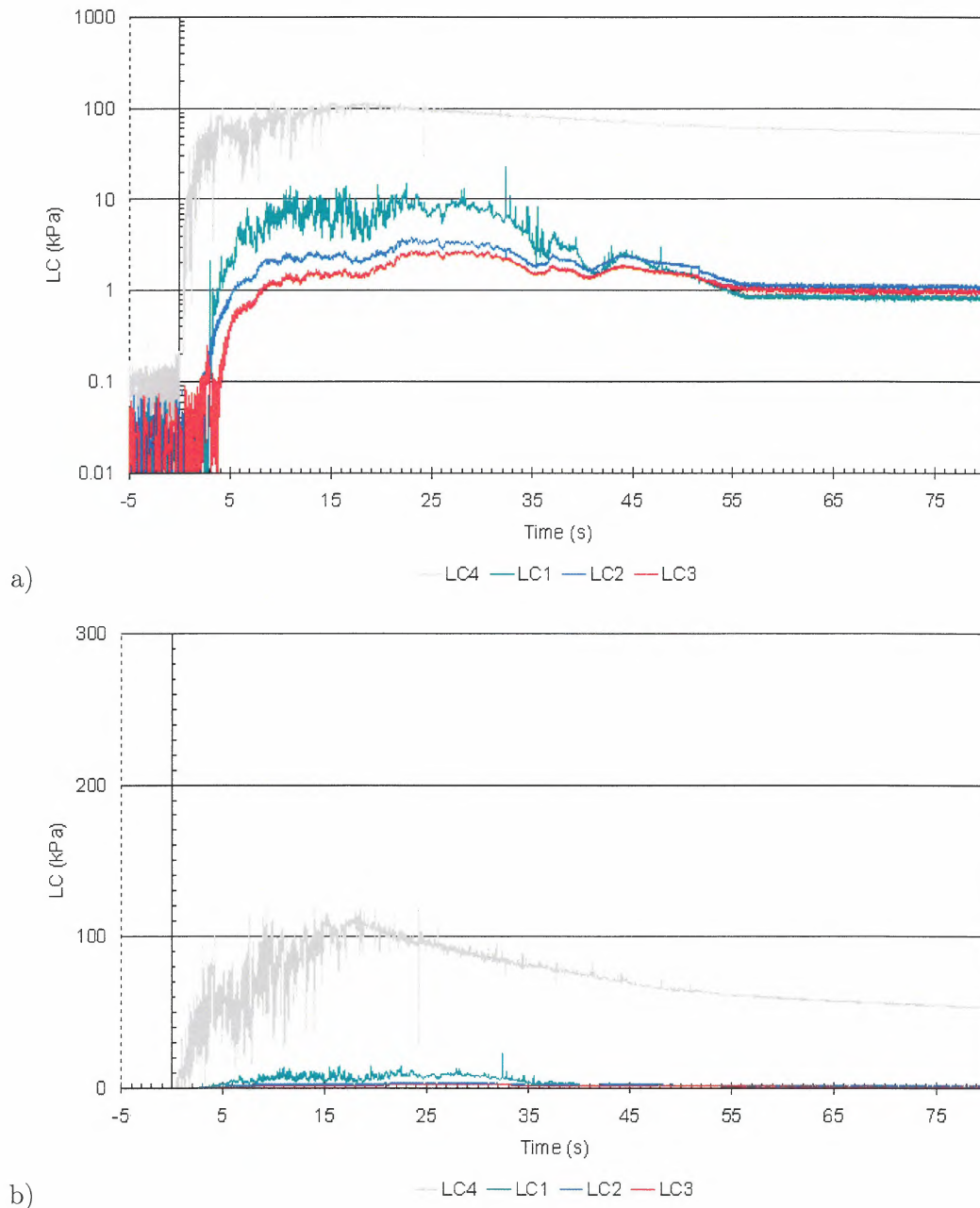


Figure 3.33: *Avalanche 20040228 15:30: Load cell measurements: pressure vs time; a) logarithmic and b) linear presentation. At this time, probably all load cell except maybe LC4 were partly or totally buried. Presented values are all reduced by an offset. Thus, the shown values for LC2, LC3 and also LC1 are basically forces transmitted through the snowpack during the avalanche passage. Offset: LC1 = 7.7 kPa, LC2 = 63.7 kPa, LC3 = 75.0 kPa.*

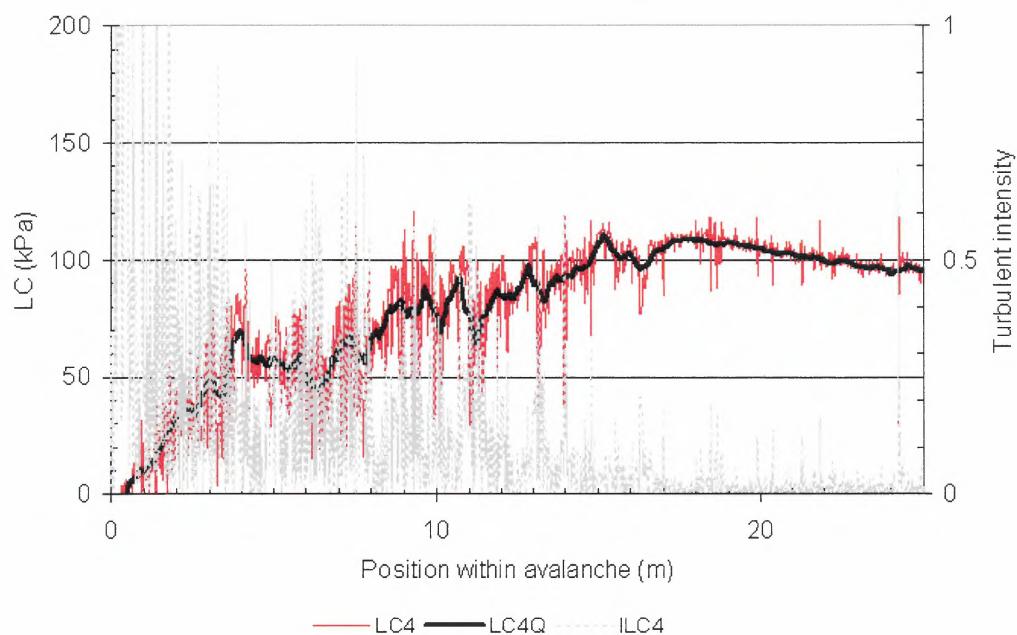


Figure 3.34: *Avalanche 20040228 15:30: Load cell measurements: pressure vs time; shown is the measured value (LC4) and a running mean (LC4Q) taken over 0.5 s (approximately between 5 m to 15 m spatial resolution). In addition, the turbulent intensity is presented (see Eq. (1.2) for definition). Obvious is a high turbulent intensity at the front of the avalanche. Shown are the first 25 s. At the tail of the avalanche ($t > 25$ s), the sensor probably got more and more buried.*

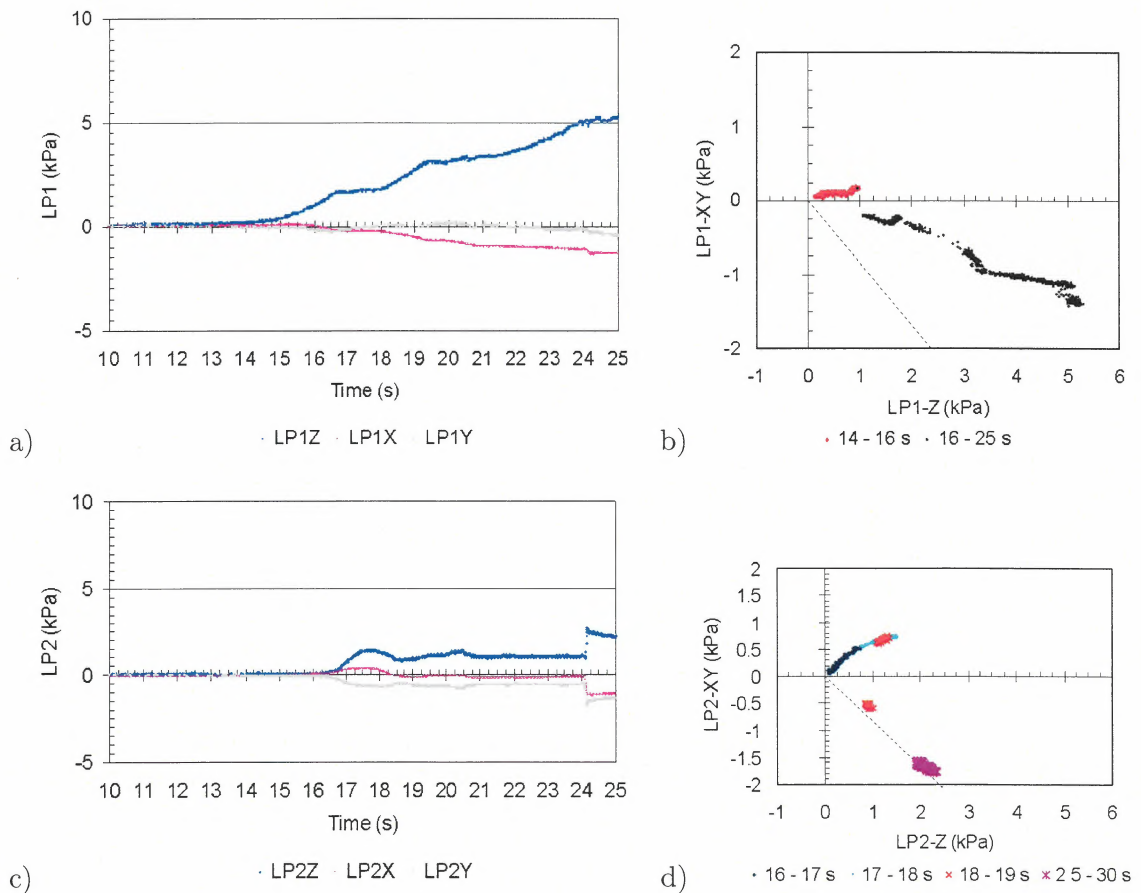


Figure 3.35: *Avalanche 20040228 15:30: Load plate measurements: a) LP1 vs time; b) LP1-XY vs LP1-Z; c) LP2 vs time; d) LP2-XY vs LP2-Z; here LP*-XY is the total shear stress and the sign indicates its direction parallel to the x-axis (see Fig. 1.1)*



References

- McClung, D. and P. Schaerer. 1993. *The Avalanche Handbook*. 1011 SW Klickitat Way, Seattle, Washington 98134, The Mountaineers.
- UNESCO/International Commission on Snow and Ice of the International Association of Hydrological Sciences, IAHS. 1981. *Avalanche Atlas*.



Appendix A – International Avalanche Classification

Contents

Table A.1	Code for morphological avalanche classification	A2
Table A.2	Canadian snow avalanche size classification system	A3



Table A.1: Code for morphological avalanche classification (1981, *Avalanche Atlas/UNESCO*)

Criterion Characteristics	Symbols		
	Criterion	Characteristics	
		pure	mixed
Manner of starting	A		
Loose snow avalanche	1	}	7
Slab avalanche	2		
Slab avalanche soft	3		
Slab avalanche soft	4		
Position of sliding surface	B		
Surface-layer avalanche (general)	1	}	7
Surface-layer avalanche, new snow fracture	2		
Surface-layer avalanche, old snow fracture	3		
Full-depth avalanche	4		
Liquid Water in snow fracture	C		
Absent: dry-snow avalanche	1	}	7
Present: wet-snow avalanche	2		
Form of Path	D		
Unconfined avalanche	1	}	7
Channelled avalanche	2		
Form of movement	E		
Powder avalanche (dominant)	1	}	7
Flow avalanche (dominant)	2		
Surface roughness of deposit	F		
Coarse deposit (general)	1	}	7
Coarse deposit angular blocks	2		
Coarse deposit rounded clods	3		
Fine deposit	4		
Liquid water in deposit	G		
Absent: dry-deposit	1	}	7
Present: wet-deposit	2		
Contamination of deposit	H		
Clean deposit	1	}	7
Contaminated deposit (general)	2		
Contaminated by rocks, debris, soil	3		
Contaminated by branches, trees	4		
Contaminated by debris of structures	5		
Triggering mechanism ¹	J		
Natural release	1		
Human release (general)	2		
Human release, accidental	3		
Human release, intentional	4		

¹This criterion is an element of the genetic classification. since the triggering mechanism within the given alternatives is known most cases and is important for many problems, it is added to the morphological code.



Table A.2: *Canadian snow avalanche size classification system and typical factors (McClung and Schaerer, 1993)*

Size	Description	Typical mass (Mg)	Typical path length (m)	Typical impact pressure (kPa)
1	Relative harmless to people	< 10	10	1
2	Could bury, injure or kill a person	10^2	100	10
3	Could bury a car, destroy a small building, or break a few trees	10^3	1000	100
4	Could destroy a railway car, large truck, several buildings, or a forest with an area up to 4 hectares	10^4	2000	500
5	Largest snow avalanche known; could destroy a village or a forest of 40 hectares	10^5	3000	1000

Kontroll- og referanseside/ Review and reference page



Oppdragsgiver/ <i>Client</i> European Commission	Dokument nr/ <i>Document No.</i> 20021048-5
Kontraksreferanse/ <i>Contract reference</i> Contract of 18.10.02	Dato/ <i>Date</i> 30 November 2004
Dokumenttittel/ <i>Document title</i> Avalanche Studies and model Validation in Europe, SATSIE	Distribusjon/ <i>Distribution</i> <input checked="" type="checkbox"/> Fri/ <i>Unlimited</i> <input type="checkbox"/> Begrenset/ <i>Limited</i> <input type="checkbox"/> Ingen/ <i>None</i>
Prosjektleder/ <i>Project Manager</i> Karstein Lied	
Utarbeidet av/ <i>Prepared by</i> Peter Gauer	
Emneord/ <i>Keywords</i> Snow avalanches, full scale tests, measurements	
Land, fylke/ <i>Country, County</i> Norway	Havområde/ <i>Offshore area</i>
Kommune/ <i>Municipality</i> Stryn	Feltnavn/ <i>Field name</i>
Sted/ <i>Location</i> Ryggefjonn	Sted/ <i>Location</i>
Kartblad/ <i>Map</i> 1418 IV Lodalskåpa	Felt, blokknr./ <i>Field, Block No.</i>
UTM-koordinater/ <i>UTM-coordinates</i> 32VMP094725	

Kvalitetssikring i henhold til/ <i>Quality assurance according to</i> NS-EN ISO9001							
Kon- trollert av/ <i>Reviewed</i> by	Kontrolltype/ <i>Type of review</i>	Dokument/ <i>Document</i>		Revisjon 1/ <i>Revision 1</i>		Revisjon 2/ <i>Revision 2</i>	
		Kontrollert/ <i>Reviewed</i>		Kontrollert/ <i>Reviewed</i>		Kontrollert/ <i>Reviewed</i>	
		Dato/ <i>Date</i>	Sign.	Dato/ <i>Date</i>	Sign.	Dato/ <i>Date</i>	Sign.
	Helhetsvurdering/ <i>General Evaluation *</i>						
KL		25/11-04	KL				
KL	Språk/ <i>Style</i>	10	KL				
KL	Teknisk/ <i>Technical</i> - Skjønn/ <i>Intelligence</i>	6	KL				
	- Total/ <i>Extensive</i> - Tverrfaglig/ <i>Interdisciplinary</i>						
PG	Utforming/ <i>Layout</i>	25.11.2004	gen				
PG	Slutt/ <i>Final</i>	25.11.2004	gen				
	Kopiering/ <i>Copy quality</i>						
* Gjennomlesning av hele rapporten og skjønnsmessig vurdering av innhold og presentasjonsform/ <i>On the basis of an overall evaluation of the report, its technical content and form of presentation</i>							
Dokument godkjent for utsendelse/ <i>Document approved for release</i>		Dato/ <i>Date</i> 30.11.2004		Sign.			